

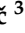







Review

Connecting Soft and Hard: An Integrating Role of Systems Dynamics in Tsunami Modeling and Simulation

Marek Zanker ¹, Bilal Naji Alhasnawi ², František Babič ³, Vladimír Bureš ^{1,*}, Pavel Čech ¹,
Martina Husáková ¹, Peter Mikulecký ¹, Tomáš Nacházal ¹, Daniela Ponce ¹, Salman Iqbal ⁴
and Bishoy E. Sedhom ⁵

- ¹ Faculty of Informatics and Management, University of Hradec Králové, 500 03 Hradec Králové, Czech Republic; marek.zanker@uhk.cz (M.Z.); pavel.cech@uhk.cz (P.Č.); martina.husakova.2@uhk.cz (M.H.); peter.mikulecky@uhk.cz (P.M.); tomas.nachazel@uhk.cz (T.N.); daniela.ponce@uhk.cz (D.P.)
- ² Department of Electricity Techniques, Al-Samawah Technical Institute, Al-Furat Al-Awsat Technical University, Kufa 66001, Iraq; bilalnaji11@yahoo.com
- ³ Department of Cybernetics and Artificial Intelligence, Faculty of Electrical Engineering and Informatics, Technical University of Košice, Letná 1/9, 042 00 Košice, Slovakia; frantisek.babic@tuke.sk
- ⁴ FOMS, Department of Management & Entrepreneurship, University of Central Punjab Lahore, Lahore 54782, Pakistan; salmaniqbal10@gmail.com
- ⁵ Electrical Engineering Department, Faculty of Engineering, Mansoura University, Mansoura City 35516, Egypt; eng_bishoy90@mans.edu.eg
- * Correspondence: vladimir.bures@uhk.cz

Abstract: Modeling and simulation have been used to study tsunamis for several decades. We created a review to identify the software and methods used in the last decade of tsunami research. The systematic review was based on the PRISMA methodology. We analyzed 105 articles and identified 27 unique software and 45 unique methods. The reviewed articles can be divided into the following basic categories: exploring historical tsunamis based on tsunami deposits, modeling tsunamis in 3D space, identifying tsunami impacts, exploring relevant variables for tsunamis, creating tsunami impact maps, and comparing simulation results with real data. Based on the outcomes of this review, this study suggests and exemplifies the possibilities of system dynamics as a unifying methodology that can integrate modeling and simulation of most identified phenomena. Hence, it contributes to the development of tsunami modeling as a scientific discipline that can offer new ideas and highlight limitations or a building block for further research in the field of natural disasters.

Keywords: tsunami; systematic review; system dynamics; modeling; software; methods



Citation: Zanker, M.; Alhasnawi, B.N.; Babič, F.; Bureš, V.; Čech, P.; Husáková, M.; Mikulecký, P.; Nacházal, T.; Ponce, D.; Iqbal, S.; et al. Connecting Soft and Hard: An Integrating Role of Systems Dynamics in Tsunami Modeling and Simulation. *Sci* **2024**, *6*, 39. <https://doi.org/10.3390/sci6030039>

Academic Editor: Claus Jacob

Received: 13 May 2024

Revised: 4 July 2024

Accepted: 9 July 2024

Published: 11 July 2024



Copyright: © 2024 by the authors. Licensee MDPI, Basel, Switzerland. This article is an open access article distributed under the terms and conditions of the Creative Commons Attribution (CC BY) license (<https://creativecommons.org/licenses/by/4.0/>).

1. Introduction

Tsunamis are potentially extremely dangerous natural hazards that occur at low frequencies and are hard to predict. The “potentiality” depends on whether the tsunami hits an uninhabited area. In this case, nothing much happens regarding direct danger to people. However, it is an extreme risk if a populated area is affected. The main issue is that the events leading up to the tsunami do not clearly indicate its origin until it is generated [1]. With frequently scarce [2], it is necessary to develop a coherent framework that incorporates existing assumptions (i.e., the system’s general model) and various methods for hazard and risk analysis in order to assess the consequences of these events on various layers of society. The underlying objective of COST Action AGITHAR (Accelerating Global Science in Tsunami Hazard and Risk Analysis) is to develop further, standardize, and document such a framework, and this document is one of the Action’s outputs. Numerous sources can generate tsunamis in the form of long propagating waves. Tsunamis are a phenomenon primarily generated along convergent margins and caused by undersea earthquakes [3]. Tsunamis, once created, travel at high speeds and cover a large area of water. In case of a large tsunami, when waves reach coastal areas, they inundate land for several kilometers.

As a result, casualties occur, as does damage to or destruction of infrastructure and built-up areas. More than 700 million people live in areas of extreme sea-level events, including tsunamis [4].

Research on tsunamis is multidisciplinary. Tsunamis can be studied from many different perspectives, namely the historical perspective, where tsunami deposits are examined, and the period when the tsunami arrived at the selected location is estimated, for example [5]. Furthermore, tsunamis are investigated from the perspective of their impact on the environment or on individual inhabited areas. Here, in particular, photo documentation is used before and after the wave impact, e.g., [6]. Another way of exploring tsunamis is their modeling, where tsunamis are usually presented as a three-dimensional environment, e.g., [7]. Models are usually developed to investigate impacts on a selected environment or on a populated area, e.g., [8], or on a hypothetical tsunami barrier, e.g., [9]. Another way of examining tsunamis is from a statistical perspective, either by searching for essential variables for the part of the tsunami being examined, e.g., [10], or from the statistical comparison of the impacts of a real tsunami with a modeled one, e.g., [11].

To date, no comprehensive systematic review has been published focusing on methods and software packages applied to explore the multidisciplinary phenomenon of the tsunami. An example of a systematic review thematically focused on tsunamis and similar events is provided by Palupi [12], who focuses on the psychological preparedness of coastal communities for a natural disaster. Fernandez et al. [13] focused on the mapping of scientific evidence on the mental health impacts of floods caused by extended periods of heavy rain in river catchments. The aim of this study is to contribute to both aforementioned topics through a deep analysis of existing modeling and simulation techniques and methods in the field of tsunami research and an outline of the possibility of further extension. The achievement of this aim is based on highlighting the importance of finding a tool that is not over-specialized and narrowly focused on particular aspects of tsunamis. While existing tools used in particular fields of study need to be applied to find answers to particular domain-related questions, the multidisciplinary nature of tsunamis requires applying a systemic approach at a higher level of complexity. The holistic view and complex structures with mutually interconnected parts represent the primary attributes of the systems approach. Hence, data or information acquired by particular tools, techniques, or modeling software can be used as inputs to more complex models, improving understanding and insights into the tsunami phenomenon. System dynamics is a commonly used methodology whose application can successfully lead to implementing the system perspective. The goal is to prove its applicability and potential added value in tsunami research.

This manuscript is structured as follows. Section 2 describes the applied methodology, which is based on a systematic review methodology, Preferred Reporting Items for Systematic Reviews and Meta-Analyses (PRISMA). Furthermore, technical details related to developing a system dynamics model are presented. The next two sections present achieved results. Section 3 provides a bibliographic analysis based on the specific keywords of identified articles. Furthermore, the results of the analysis of different types of software and methods for tsunami research are presented. Section 4 describes the developed system dynamics model, which demonstrates how various aspects can be integrated by one methodological approach. Particular modules are introduced. The final section concludes the paper with an outline of existing limitations and potential research pathways. Finally, the appendices capture an enumeration of the individual software applications, their methods, and reasons for their use. Moreover, an overview of the relationships between the software and the scientific disciplines and technical details associated with the developed model are provided.

2. Materials and Methods

2.1. Literature Analysis

Collecting a data set that might be used for further analysis was the initial step in the study. To conduct a review, one can choose from two alternatives. The first option

involves looking for relevant information resources in databases maintained by individual publishing houses (Elsevier, Springer, Wiley, etc.). The second approach uses databases that have selected journals indexed (Web of Science, Scopus, EBSCO, etc.). Both strategies have advantages and disadvantages. The former, for example, provides a data collection from a broader set of resources, but the latter works with publications whose quality is recognized by authority and a community. We found the latter more suitable for this study due to the absence of redundant records. Thus, a search in the Web of Science database for published papers was conducted.

Articles focused on tsunamis that used software for this activity represented the target of the search. The main criteria for searching articles were the language used, namely English; the year of publication, between 2010 and 2020; full-text availability (in order to conduct the content analysis); and the use of a software package for tsunami exploration. Initially, we intended to use the following search command for the intended systematic search:

2.1.1. Tsunami (Topic)

Refined by: Document Types: Articles, Publication Years: 2023 or 2022 or 2021 or 2020 or 2019 or 2018 or 2017 or 2016 or 2015 or 2014 or 2013 or 2012 or 2011 or 2010

However, articles containing the term “tsunami” broadly did not refer to tsunamis in the true sense of the word. An example of this phrase might be the tsunami of obesity. Therefore, we decided to narrow the search. The additional concept “water” filtered out articles that were not focused on the topic of this systematic search. Thus, we used the following command:

2.1.2. Tsunami (Topic) and Water (Topic)

Refined by: Document Types: Articles, Publication Years: 2023 or 2022 or 2021 or 2020 or 2019 or 2018 or 2017 or 2016 or 2015 or 2014 or 2013 or 2012 or 2011 or 2010

The next step was to search for full-text versions of the articles. This step does not follow the exact PRISMA methodology [14]; however, due to the search for software used in the tsunami field and also the lack of a list of software used in the tsunami field, we decided to skip the abstract screening step. Another reason for skipping this stage is that applied software applications are not always mentioned in abstracts.

Consequently, we searched for the word “software” in the full-text versions of the articles. We used Adobe Acrobat Reader DC [15] software for the search. We recorded the name of each software found and entered it into the list of used software. After we had searched all available articles, we started a new search using the aforementioned software, which included the software names found in the previous full-text search. In this step, we sorted the articles based on those in which some of the found software was used and those in which it was not. We then searched the articles in which tsunami software was used (if the article did not use one of the found software, it was omitted with Reason 1). We then excluded articles from this set of articles that did not have a specific method (if the article did not use one of the found methods, it was omitted with Reason 2). The whole process is shown in Figure 1. Eventually, we found 2015 articles, from which we included 1573 in the full-text search, and 105 articles passed the full-text screening.

As a part of the analytical section of the systematic review, we performed a bibliographic synthesis of keywords using the VOSviewer [16] tool. Seventeen articles were not included in this stage due to failure to include keywords in the articles. Linguistic word preparation was conducted in which, for instance, keyword run-up and run-up were unified under the single term run-up, or the keyword tsunami was excluded from the synthesis because of the focus of all the articles on this topic. Moreover, the exclusion was necessary as we tried to answer the following research questions: (1) What software tools and methods are used in tsunami research? and (2) How are tsunami research tools interconnected?

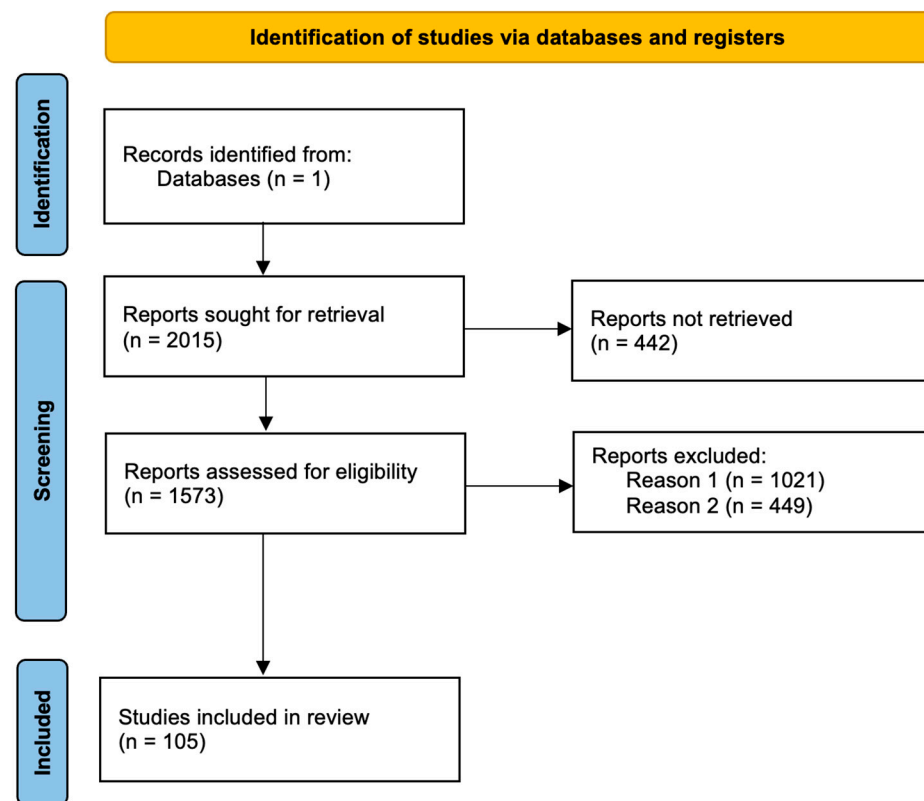


Figure 1. PRISMA stages (own work; template adopted from [14]).

2.2. Model Development

System dynamics represents a specific and original methodological approach to modeling and simulating various types of systems. The core concepts of systems thinking, such as interconnectedness, feedback, adaptive capacity/resilience, self-organization, and emergence [17], are applied in system dynamics to help people make better decisions when confronted with complex, dynamic systems. The field provides a philosophy and tools to model and analyze dynamic systems.

Differential and difference equations are traditionally used to represent change in dynamic systems. However, system dynamics provides an intuitive modeling language, which is typical for all applications. This makes system dynamics an ideal tool for multidisciplinary work [18] as it enables the integration of subsystems that are distinct in their fundamental essence, i.e., soft disciplines such as economics or psychology can be connected with hard disciplines such as physics or geology. Exploration of complex phenomena such as tsunamis represents an appropriate example. Therefore, a complex model of various aspects of a tsunami has been developed to demonstrate the benefits and added value of incorporating this methodology into this field of study.

This study presents an original model presenting possibilities of tsunami analysis. The process of model development was based on the following procedure:

- Identification of key topics in the scientific literature based on the literature review;
- Classification of variables into distinct groups to develop particular model sectors or modules;
- Identification of causal links among variables and feedbacks, i.e., causal loop diagrams;
- Determination of time units (hours);
- Transformation to a simulable model, i.e., development of stock and flow diagrams;
- Performance of model validation tests [19]—structural validity (boundary adequacy, parameter verification, dimensional consistency) and behavioral validity (behavior pattern test, extreme condition test, sensitivity test).

3. Results

3.1. Application of Methods and SW Tools in the Current Research of Tsunamis

Figure 2 reveals that single methods or techniques are used mostly separately in research. One cluster is connected with the consequences of tsunamis in the form of numerical simulations that are primarily applied in the analysis of technical issues, such as construction vulnerability, and environmental issues, such as the influence of the tsunami wave on vegetation. The second cluster includes numerical modeling as well. This context deals with the origin of a tsunami and the wave itself. However, based on the discrepancy between the results from Table 1 presented below, where the interdependence of software tools usage reached a higher level, we decided to augment the input data with the name of the tool used. Thus, we added the names of the tools used to the keywords already provided by the authors of the articles. Then, we created a new outcome of the bibliographic analysis with the same settings as for the previous one. The results are presented in Figure 3. It is clear that most of the specific tools used in the tsunami field are interrelated. In fact, there is only one huge cluster and a few solitary outliers. It reveals that the applied methods are integrated mainly by the usage of OpenFoam, Matlab, and Calib.

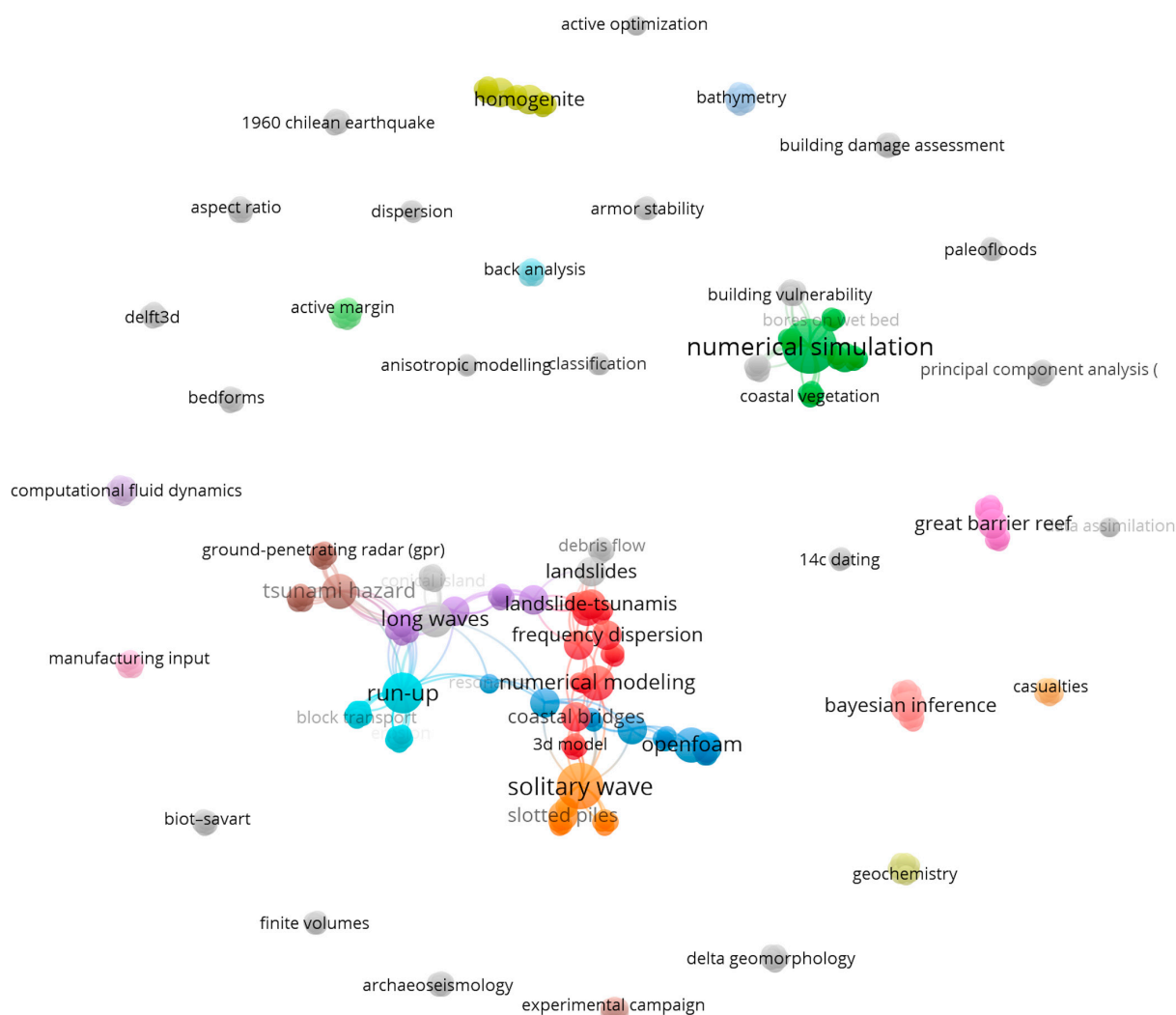


Figure 2. The interconnectedness of methods and techniques. Note: This figure shows the interconnectedness of the keywords mentioned in the analyzed articles. In the figure, there is one larger cluster mainly focused on modeling and many smaller clusters that refer to the specifics of different models (own work; software: VOSviewer [16]).

Table 1. SW tools and research methods were applied to analyzed studies.

Author(s) and Year	Citation	Software	Methods	Application
Liu et al., 2020	[20]	OpenFOAM	CFD, FAM, FVM, MULES, PIMPLE	To simulate breaking wave-induced seabed scour and coastal erosion. It aims to understand and evaluate nearshore tsunami deposit transport processes, particularly around offshore structures like monopiles.
Qin, Motley, LeVeque, et al., 2018	[21]	GeoClaw, OpenFOAM	CFD, NSWE, PISO, VOF	Compares GeoClaw, a 2D depth-integrated model, and OpenFOAM, a 3D model based on tsunami inundation modeling.
Autret et al., 2016	[22]	Agisoft, ArcGIS	DEM	Investigates large clastic cliff-top storm deposits on Banneg Island during the stormy winter of 2013–2014 to understand the impacts of extreme storm waves on rocky coasts.
Xiong et al., 2019	[23]	HAZUS	DEM, SWE	presents a deterministic approach for assessing large-scale building damage from tsunamis by quantifying lateral loading on structures induced by tsunami waves. Utilizing a depth-averaged hydrodynamic model that solves 2D nonlinear shallow water equations.
Bellotti, 2020	[24]	MATLAB	FEM	Model for evaluating long wave amplification in coastal areas using a modal decomposition method to amplify natural modes under forcing waves.
Abril and Periañez, 2017	[25]	MATLAB	FFT	Presents numerical simulations of the tsunami triggered by the 1995 Nuweiba earthquake in the Gulf of Aqaba, aligning well with available observations. It explores 12 potential tsunamigenic sources in the Red Sea.
Yao et al., 2020	[26]	OpenFOAM	CFD, MULES, PIMPLE, VOF	Enhance the understanding of tsunami-like solitary wave run-up reduction by pile breakwaters on a sloping beach, a 3D numerical wave tank.
Tan et al., 2018	[27]	Delft3D	SPH	Introduces a numerical landslide-tsunami hazard assessment technique applicable to reservoirs, lakes, fjords, and seas.
Knighton and Bastidas, 2015	[28]	Delft3D	MONTE CARLO, PTHA	Enhances existing probabilistic tsunami hazard analysis by differentiating between epistemic and aleatory uncertainties.
Horrillo et al., 2013	[29]	FLOW3D	CFD	Introduces and validates TSUNAMI3D, a simplified 3D Navier–Stokes model designed for computational efficiency for simulating water and landslide interactions.
Kevlahan et al., 2015	[30]	MATLAB	GKS, MOST	Introduces a new mass and energy-conserving Brinkman penalization for the rotating Shallow Water Equations, designed to enforce solid-wall boundary conditions with complex coastlines easily.
Aristodemo et al., 2020	[31]	OpenFOAM	CFD, VOF	Investigates the hydrodynamic forces exerted by solitary waves on horizontal circular cylinders near a rigid bed through experimental and numerical methods.
Wang and Liu, 2011	[32]	COMCOT	LSWE, NSWE	Modifying leap-frog finite difference scheme to solve Nonlinear Shallow Water Equations.
Völker et al., 2011	[33]	MB-System	DEM	Compares bathymetric datasets from before and after the Mw 8.8 Maule Earthquake on 27 February 2010 offshore Central Chile, finding no new submarine landslides more enormous than 1 km as a direct consequence of the earthquake.
Flouri et al., 2013	[34]	ArcGIS	DEM, NSWE	Employs a splitting method to reduce the hyperbolic system into two successive systems, solving the equations with a dispersive.
Restrepo A, 2012	[35]	DSAS	DEM	Examines the physical and human-induced factors influencing the recent evolution of the Patía River delta.
Giraldi et al., 2017	[36]	GeoClaw	MAP, MONTE CARLO	Focuses on estimating earthquake model parameters through the resulting tsunami, specifically applied to the 2010 Chile event.
Stefanakis et al., 2014	[37]	VOLNA	NSWE	Investigates whether small islands near the mainland offer protection from tsunamis.
Abril-Hernández et al., 2018	[38]	QGIS	DEM	Analyzes the outflow dynamics of Lake Bonneville breached at the Marsh Creek Fan.
Mehrotra et al., 2015	[39]	MATLAB	FCM, PCA	The proposed method involves image classification with a radial basis function neural network and a generalized improved fuzzy partition FCM algorithm.
Amante, 2018	[40]	MB-System	DEM	To develop and apply a methodology for estimating and mapping vertical errors in integrated bathymetric–topographic DEMs along coastal regions.
Mitsui et al., 2016	[41]	OpenFOAM	CFD	Analyze the fluid forces acting on the armor blocks during tsunami overflow.
Zhu and Dong, 2020	[42]	ANSYS	CFD	Through laboratory experiments and CFD analysis, investigate the vertical and horizontal forces induced by solitary waves on coastal bridges.
Förster et al., 2010	[43]	CALIB	AMS	To understand the previous failure events and current hazard potential of the Mauritania Slide Complex along the NW-African continental margin.

Table 1. Cont.

Author(s) and Year	Citation	Software	Methods	Application
Puga-Bernab�u et al., 2017	[44]	ArcGIS, Fledermaus	AMS, DEM	To investigate the geomorphologic characteristics and evolutionary processes of the Gloria Knolls Slide complex on the Great Barrier Reef margin.
Bourget et al., 2010	[45]	CALIB	AMS	To investigate the growth and evolution of the Late Quaternary turbidite system along the Makran convergent margin through high-resolution stratigraphy from deep-sea cores.
Smith et al., 2010	[46]	CALIB	AMS	To examine the changes in relative sea level and their impact on human activity distribution in the Forth lowland, Scotland, from approximately 11,700 to 2000 calibrated years before the present.
Baumann et al., 2017	[47]	Agisoft	DEM	Analyzing washover deposition processes and distinguishing between storm and tsunami overwash events by examining the washover deposits from the exceptional wave climate during the winter of 2013–2014 in the Bay of Biscay.
Ali et al., 2019	[48]	ANSYS	VOF	To investigate the role of inland vegetation in reducing the energy of flood flows and minimizing structural damage.
Torres et al., 2019	[49]	COMCOT	NSWE, LSWE	To investigate tsunami-induced magnetic field disturbances by comparing observed magnetic records with computed magnetic fields for the 2010 and 2015 Chilean tsunamis.
Polonia et al., 2013	[50]	CALIB	AMS	To re-evaluate the origin of the 20–25 m thick megaturbidite (Homogenite/Augias) in the Ionian Sea through geophysical surveys and sediment cores.
Dutykh and Clamond, 2016	[51]	MATLAB	FVCF, NSWE	To propose a modified version of the NSWE for modeling irrotational surface waves under significant bottom variations in space and time.
Jing et al., 2012	[52]	Amira	SWE	To develop a numerical model to simulate the behavior characteristics of harbor waves and investigate resonance phenomena.
Jiang et al., 2019	[53]	OpenFOAM	CFD, MULES, PIMPLE, PISO, SIMPLE, VOF	To numerically examine the effects of tsunami-like hydrodynamic loading on free-standing structures with various architectural geometries using a multiphase numerical model based on the volume of fluid method in three-dimensional space.
Sarjamee et al., 2017	[54]	OpenFOAM	CFD, FVM, VOF	To present and validate a fully coupled (hydrodynamic and morphologic) numerical model based on the open-source CFD package OpenFOAM, designed to simulate flow and morphology changes induced by a solitary wave on a sloping beach.
Li et al., 2019	[55]	OpenFOAM	CFD, VOF	
Ruffini et al., 2019	[56]	Delft3D, MATLAB	SPH	Using the hydrodynamic numerical model, quantify the effect of water body geometry on the propagation of large landslide tsunamis in the far field.
Wijetunge, 2010	[57]	COMCOT	SWE	To outline the field measurements and numerical modeling conducted to develop a high-resolution tsunami inundation map for Trincomalee on the east coast of Sri Lanka, which was heavily affected by the 2004 tsunami.
Ulvrova et al., 2014	[58]	COMCOT	NSWE	To assess tsunami hazards from underwater volcanic explosions by simulating tsunamis generated from a submerged vent in Karymskoye Lake, Kamchatka, and the Kolumbo submarine volcano near Santorini, Greece.
H. Zhang et al., 2019	[59]	HydroSed2D	NSWE	To investigate the damping effect of vegetation, specifically Pandanus odoratissimus, on tsunami wave run-up and land inundation on coastal beaches.
Kevlahan et al., 2019	[60]	MATLAB	SWE	To address the problem of optimally determining the initial conditions for the one-dimensional SWE in an unbounded domain using a limited number of sea surface height observations.
Douglas and Nistor, 2015	[61]	OpenFOAM	CFD, FVM, PISO	To investigate the propagation and structural interaction of tsunami-like bores using a multiphase three-dimensional numerical model.
Bartzke et al., 2016	[62]	MATLAB	SPH	To understand the hydrodynamic processes and tsunami deposit transport in gravel-dominated coastal environments, where storm waves, spring tides, bore waves, and tsunamis can form gravel bedforms.
San Pedro et al., 2017	[63]	CALIB	AMS	To provide a new interpretation of the Augias deposit in the Ionian Sea, focusing on its sedimentary processes and origins.
Premasiri et al., 2015	[64]	MATLAB	GPR	To evaluate and mitigate tsunami hazards by reconstructing past tsunamis using coastal sediments deposited by tsunamis.
Cheff et al., 2019	[65]	ArcGIS	DEM	To evaluate the risks and evacuation needs associated with a potential near-field tsunami event from the Cascadia subduction zone, focusing on the Town of Tofino on Vancouver Island’s West Coast.

Table 1. Cont.

Author(s) and Year	Citation	Software	Methods	Application
X. Zhang and Niu, 2020	[66]	ArcGIS	DEM, MONTE CARLO, PTHA	To develop a more efficient approach to probabilistic tsunami hazard assessment that balances accuracy and feasibility. Traditional methods require many scenario simulations to account for uncertainties in seismic parameters.
Juran et al., 2019	[67]	OsiriX DICOM	PCA	To examine the factors influencing the adoption of latrines provided during post-2004 tsunami reconstruction efforts in India.
Sraj et al., 2017	[68]	tsunami-2d	MONTE CARLO	To present an efficient method for inferring the fault slip distribution of the Tōhoku earthquake using water surface elevation data.
Triantafyllou et al., 2019	[69]	GeoClaw, MATLAB	MAP, MONTE CARLO	To conduct a comprehensive tsunami risk assessment for a coastal segment west of Heraklion, Crete, by considering the convolution of tsunami hazard, vulnerability of assets (e.g., buildings), and the economic value exposed.
Chen et al., 2020	[70]	Geowave	DEM	To propose using reciprocal Green's functions (RGFs) as an effective tool for forecasting tsunamis generated by submarine landslides, which can sometimes produce higher waves than seismic tsunamis in areas close to the source and are more challenging to predict.
Reinhardt et al., 2010	[71]	CALIB	AMS	To predict the recovery time of the Río Cruces to pre-1960 conditions following the significant subsidence caused by the 22 May 1960 Chilean earthquake, the largest on record with a magnitude of 9.5.
Stefanakis et al., 2015	[72]	VOLNA	NSWE	To study the extreme characteristics of the run-up of transient long waves.
Álvarez-Gómez et al., 2011	[73]	COMCOT	MONTE CARLO	To model the tsunami impact on the Spanish and North African coasts of the Alboran Sea, generated by several reliable seismic tsunamigenic sources in the area.
Çağatay et al., 2012	[74]	CALIB	AMS	To analyze sedimentary earthquake records from the last 2400 years in the central Karamürsel Basin of the Izmit Gulf, located in the eastern Sea of Marmara.
Dahanayake et al., 2012	[75]	CALIB	AMS	To analyze the sediments deposited by the 2004 Sumatra–Andaman tsunamigenic earthquake in various coastal and inland locations of Sri Lanka.
Vött et al., 2010	[76]	CALIB	AMS	To present evidence of multiple tsunami impacts on the Bay of Palairos-Pogonia, NW Greece, during the Holocene, based on detailed geoscientific studies.
Yakupoglu et al., 2019	[77]	CALIB, R-studio	AMS	To examine the Holocene earthquake history of the Central High Segment of the North Anatolian Fault by analyzing seismoturbidities within a 21 m long piston core recovered from the Kumburgaz Basin in the Sea of Marmara.
Stiros and Blackman, 2014	[78]	CALIB	AMS	To shed light on the sequence of coastal uplift and subsidence along the coasts of Rhodes Island, mainly focusing on archaeological evidence from a 2400-year-old harbor currently about 3 m above sea level.
Ma et al., 2019	[79]	ICEM, OpenFOAM	PIMPLE, VOF	To present a more accurate method for predicting the maximum run-up height and inundated area caused by tsunami events.
Sarfraz and Pak, 2017	[80]	OpenFOAM	SPH	To numerically derive tsunami wave loads on bridge superstructures using smoothed particle hydrodynamics.
Yang et al., 2020	[81]	ANSYS	CFD, VOF	To investigate the generation mechanism and characteristics of peak values of tsunami bore vertical force on a scaled-down two-dimensional T-girder model.
Webster et al., 2016	[82]	ArcGIS	AMS	To investigate shallow submarine landslides along the central Great Barrier Reef and their potential to produce tsunamis.
Fabregat et al., 2019	[83]	CALIB, reflexW	AMS, GPR	To demonstrate the practicality of integrated studies combining trenching, numerical dating, and shallow geophysical techniques to characterize the subsurface subsidence structure associated with sinkholes and reconstruct their deformational and sedimentary history.
Gylfadóttir et al., 2017	[84]	GeoClaw	DEM, SWE	To analyze and model the tsunami generated by a giant rockslide that occurred on 21 July 2014 from the inner Askja caldera into Lake Askja, Iceland.
Higman et al., 2018	[85]	QGIS	DEM	To analyze the catastrophic slope failure at the terminus of Tyndall Glacier on 17 October 2015, which sent 180 million tons of rock into Taan Fiord, Alaska.
Xing et al., 2016	[86]	Gambit	CFD, DEM, VOF	To analyze and simulate the catastrophic rock avalanche that occurred at about 8:30 p.m. on 27 August 2014 in Fuquan, Yunnan, southwestern China.
Dall'Osso et al., 2014	[87]	ArcGIS	DEM, MOST	To conduct a PTHA for the Sydney metropolitan area, addressing the significant gap in published PTHAs, including inundation for Australia.
Xie and Chu, 2019	[88]	OpenFOAM	VOF	To investigate the hydrodynamic forces on coastal structures impacted by tsunamis, focusing on the effects of the wave Froude number, the sizes and shapes of the structures, and the initial conditions.

Table 1. Cont.

Author(s) and Year	Citation	Software	Methods	Application
Creach et al., 2015	[89]	SPAD	MONTE CARLO, PCA	To address the lessons learned from Storm Xynthia in February 2010, which caused a significant sea surge along the French Atlantic coast, flooding low-lying coastal areas, particularly urbanized regions.
Qin, Motley, and Marafi, 2018	[90]	OpenFOAM	CFD	To enhance the understanding of tsunami inundation impacts on coastal communities, high-resolution 3D CFD modeling will be incorporated to simulate tsunami overland flow around existing macro-roughness features such as buildings and bridges.
Álvarez-Gómez et al., 2013	[91]	COMCOT	NSWE	To assess tsunami hazards along the coast of El Salvador, the smallest and most densely populated country in Central America.
DeDontney and Rice, 2012	[92]	COMCOT	FFT	To resolve the disparity in tsunami lead wave morphologies observed by two satellites.
Cariolet, 2010	[93]	ArcGIS	DEM	To map and analyze the coastal areas in western Brittany that were inundated during a storm on 10 March 2008
Boshenyatov and Zhiltsov, 2019	[94]	OpenFOAM	PISO, VOF	To investigate the energy losses of tsunami-like waves due to the formation of large eddies near underwater barriers, an area of growing importance.
Reynolds et al., 2015	[95]	ArcGIS, Delft3D	DEM	To assess the impact of sea-level rise and wave-driven flooding on seabird colonies in the Pacific, mainly focusing on a globally important seabird rookery at Midway Atoll in the subtropical Pacific.
Benazir et al., 2023	[96]	COMCOT	SWE	To reflect on the progress of tsunami preparedness in a coastal community in Aceh, Indonesia, nearly two decades after the catastrophic 2004 Indian Ocean tsunami.
Rauter et al., 2021	[97]	OpenFOAM	CFD, PISO, MULES	To evaluate the performance of the multiphase Navier–Stokes equations implemented in OpenFOAM for simulating impulse wave generation by landslides.
Nemati et al., 2023	[98]	ArcGIS, MATLAB	DEM	To report the results of numerical simulations for a potential subaerial landslide on the coast of Orcas Island and the resultant tsunami waves in the southern Strait of Georgia.
Guo and Lo, 2022	[99]	OpenFOAM	CFD, PIMPLE, VOF	To investigate the hydrodynamics of a solitary wave passing a vertical cylinder over a viscous mud bed for the first time.
Attili et al., 2021	[100]	OpenFOAM	FVM, PIMPLE, VOF	To focus on the numerical modeling of landslide tsunamis impacting dams.
Pakoksung et al., 2021	[101]	QGIS	DEM, PTHA	To perform a probabilistic hazard analysis of a tsunami generated by a subaqueous volcanic explosion at Taal Lake, located on Luzon Island in the Philippines.
Song et al., 2023	[102]	OpenFOAM	VOF	To investigate the impacts of tsunami-like waves on coastal bridge decks with superelevation, addressing a gap in existing research that typically focuses on wave impacts on flat bridge decks.
Elsheikh et al., 2022	[103]	OpenFOAM	CFD, FVM	To investigate the hydrodynamics of turbulent bores that propagate on a horizontal plane, closely resembling dam-break waves and tsunami-like hydraulic bores.
Rahuman et al., 2022	[104]	ANSYS	CFD	To visualize and compare the fluid flow patterns around the Rhizophora mangrove species' stilt roots and the Avicennia mangrove species' pneumatophore roots in the Pichavaram mangrove forest.
Amina and Tanaka, 2022	[105]	ANSYS	CFD, VOF, SIMPLE	Using numerical simulations to predict how Free Surface Level variations around finite-length vegetation affect flow structure.
Liu and Hayatdavoodi, 2023	[106]	OpenFOAM	VOF, CFD	To investigate the impact of waves and bores generated by broken solitary waves on horizontal decks of coastal structures.
Paulin et al., 2022	[107]	MATLAB	MAP	To enhance the 4D-Var method for filtering partially observed nonlinear chaotic dynamical systems by improving the accuracy of the initial condition estimation and subsequent propagation via model dynamics.
Kalligeris et al., 2022	[108]	Agisoft, ArcGIS	DEM	To infer complete tsunami hydrographs from field measurements and to report the first wave arrival timing, polarity information, and tsunami height/run-up measurements for five islands.
Tong et al., 2023	[109]	MATLAB	MAP	To compute the probability of tsunamis reaching a certain size on shore based on earthquake-induced seafloor elevations.
Dai et al., 2021	[110]	QGIS	DEM	To simulate the formation of a weak layer in the mountainous slope leading to the Taan Fiord landslide and to analyze the triggering factors from a geotechnical engineering perspective.
Madden et al., 2023	[111]	GeoClaw	DEM	To leverage Google's Tensor Processing Unit to rapidly evaluate different tsunami risk mitigation strategies, making high-performance computing accessible to communities.
Yuan et al., 2021	[112]	COMCOT	PTHA, NSWE, LSWE	To conduct a PTHA for mainland China and Taiwan Island.
Celikbas et al., 2023	[113]	ArcGIS	DEM	To assess tsunami evacuation planning for the Bodrum district along Turkey's western coast, which faces significant tsunami risks due to the active seismicity in the Eastern Mediterranean Sea.

Table 1. *Cont.*

Author(s) and Year	Citation	Software	Methods	Application
Zengaffinen-Morris et al., 2022	[114]	ArcGIS	PTHA	To address the challenges in PTHA related to submarine landslides, which have been less explored than earthquake sources.
Mokhtarzadeh et al., 2022	[115]	OpenFOAM	VOF, CFD	To present numerical simulations of impulsive waves generated by various landslides, including solid block, granular materials, and heavy block sinking.
Mu et al., 2023	[116]	OpenFOAM	CFD, VOF, SIMPLE, PIMPLE, PISO	To investigate a three-dimensional dam-break flow scenario interacting with vertical circular and square cylinders using computational fluid dynamics simulations.
Dai et al., 2023	[117]	OpenFOAM	SPH	To investigate submarine landslide tsunamis, a significant global geohazard.
Zhang et al., 2021	[118]	MATLAB	SWE	To develop a numerical method, specifically a rezoning-type adaptive moving mesh discontinuous Galerkin method, for accurately solving the Shallow Water Equations over non-flat bottom topography.
Ersoy et al., 2022	[119]	ArcGIS	VOF, CFD	To assess the potential risk posed by impulse waves originating from concurrent landslides in Çetin Dam Reservoir in Southeast Turkey, located near an active orogenic belt.
Paris et al., 2021	[120]	OpenFOAM	CFD, PIMPLE, PISO, SIMPLE	To model tsunamis generated by granular landslides.
Lo Re et al., 2022	[121]	MATLAB, QGIS	PTHA, DEM	To assess and quantify the vulnerability of buildings in Marzamemi, Sicily, to tsunami hazards.
Takegawa et al., 2023	[122]	OpenFOAM	PISO, VOF	To investigate optimal dike shapes to mitigate tsunami overflow, focusing on numerical simulations based on waveforms from the Great East Japan Earthquake.

Table 1 presents a synthesis of the included articles in the systematic review. The reason for each tool is provided. In Appendix A, Table A1, each tool is described; the descriptions are based on the official sources of each tool. The tools we found include OpenFOAM, CALIB, MATLAB, ArcGIS, COMCOT, Delft3D, GeoClaw, ANSYS, Agisoft, MB-System, QGIS, Tsunami-2d, VOLNA, Amira, DSAS, Fledermaus, FLOW3D, Gambit, Geosoft Oasis, Geowave, HAZUS, HydroSed2D, ICEM, OsiriX DICOM, R-studio, reflexW, SPAD. In Appendix A, Table A2 captures the transposed usage for each method, respectively, for all method usage in the articles we analyzed. The methods we found include the following: Accelerator Mass Spectrometry (AMS), Computational Fluid Dynamics (CFD), Constant Rate of Supply method (CRS), Digital Elevation Models (DEM), Finite Area Method (FAM), Fuzzy C-Means Clustering (FCM), Finite Element Mesh (FEM), Fast Fourier Transform (FFT), Finite Volume with Characteristic Flux (FVCF), Finite Volume Method (FVM), Gustafsson–Kreiss–Sundström stability theory (GKS), Ground-Penetrating Radar (GPR), Linear Shallow Water Equations (LSWE), Maximum a posteriori values (MAP), MONTE CARLO (MC), Method for Splitting Tsunamis (MOST), Multidimensional Universal Limiter for Explicit Solution (MULES), Nonlinear Shallow Water Equations (NSWE), Principal Component Analysis (PCA), Pressure Implicit with Splitting of Operator (PIMPLE), Pressure Implicit with Splitting of Operators (PISO), Probabilistic Tsunami Hazard Analysis (PTHA), Semi-Implicit Method for Pressure-Linked Equations (SIMPLE), Smoothed Particle Hydrodynamics (SPH), Shallow Water Equations (SWE), and volume of fluid (VOF).

Based on Tables 1 and A1 presented in Appendix A, two types of the most numerous tsunami-related models can be identified, namely, models that directly model tsunamis or parts of tsunamis and models aimed at identifying events in history based on tsunami deposit examination.

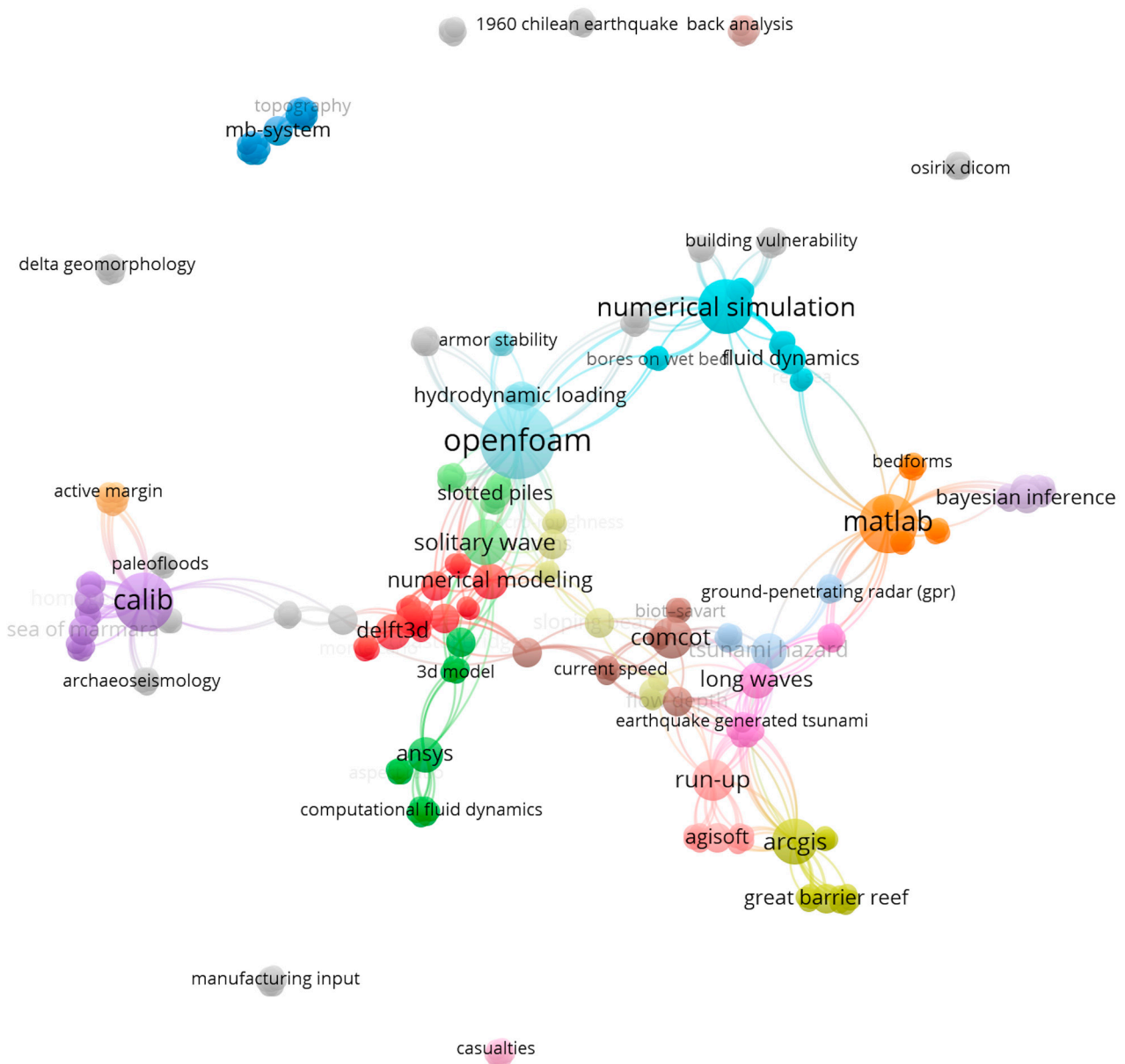


Figure 3. The interconnectedness of methods, tools, and SW applications with their tools. Note: This figure shows the interconnectedness of using the different tsunami modeling tools. Unlike the previous figure focusing on keywords, the individual tools are quite significantly interconnected (own work; software: VOSviewer [16]).

Table 2 shows the selected ratio of software use to the scientific disciplines (categories in which articles are classified in WoS) in which the articles were published (the whole table is in Appendix A, Table A3). As the Pareto rule of thumb suggests, 80.1% of software use belongs to 8 (30.8%) individual software. The situation is similar in the scientific fields, where 80.3% of the software used falls into 10 (34.5%) scientific fields related to tsunamis.

As mentioned earlier and shown in Figure 3, the different tsunami tools are interrelated. This interdependence is also evident in the scientific fields in which the papers were published. OpenFOAM (used in 32% of total cases) is the most multidisciplinary software application. For example, the MATLAB tool (used in 13.1% of total cases) was expected to be applied in various domains because of the multidisciplinary use of the tool in general. Surprisingly, the multidisciplinary application was not expected in the case of the CALIB tool (used in 8.6% of total cases). However, the results revealed the contrary.

Table 2. Application of SW tools in particular research domains.

	OpenFOAM	ArcGIS	MATLAB	COMCOT	CALIB	ANSYS	DelFT3D	QGIS	GeoClaw	Agisoft	Total
Geosciences, Multidisciplinary	3	8	4	5	8	0	1	3	3	0	35
Oceanography	8	5	3	1	3	2	1	1	1	2	27
Engineering, Ocean	16	1	4	1	0	2	2	1	0	0	27
Engineering, Civil	10	1	3	1	0	3	1	1	0	0	20
Water Resources	6	4	1	3	1	0	1	1	1	0	18
Meteorology and Atmospheric Sciences	3	3	2	3	1	0	1	0	1	0	14
Engineering, Marine	8	0	2	0	0	2	1	1	0	0	14
Geochemistry and Geophysics	0	0	3	3	1	0	0	0	1	0	8
Engineering, Multidisciplinary	2	0	1	0	0	1	0	0	0	3	7
Multidisciplinary Sciences	0	2	0	0	1	0	1	1	0	0	5
Total	56	24	23	17	15	10	9	9	7	5	

Note: These are selected fields and tools. For an overall overview, see Appendix A, Table A3. The fields of each article are retrieved from WoS. The number of fields varies for each article.

3.2. SD Model of Tsunami-Related Phenomena

As it is clear from the literature analysis, various methods and tools are used in tsunami research. However, system dynamics tools, particular software applications, or methods are not used. The reason is apparent. Applied techniques, tools, and software packages focus on a specific domain or set of issues. They enable highly specialized modeling and simulation. The aim of this section is to demonstrate the suitability of the system dynamics methodology for modeling and simulation of various aspects of tsunamis and the mutual interconnection of soft and hard disciplines. Hence, a model of tsunami-oriented aspects has been developed. The model contains seven main subsystems (modules), which represent topics under study, namely the module describing the tsunami as a natural phenomenon (The formation of the Tsunami) and six other modules showing the spheres affected by the tsunami wave, namely the modules People, Buildings, Infrastructure, Finance, Defensive elements, and Environment. Apparently, modules can be extended by any aspect we need to investigate. This configuration is created only for demonstrative purposes.

3.2.1. The Formation of the Tsunami

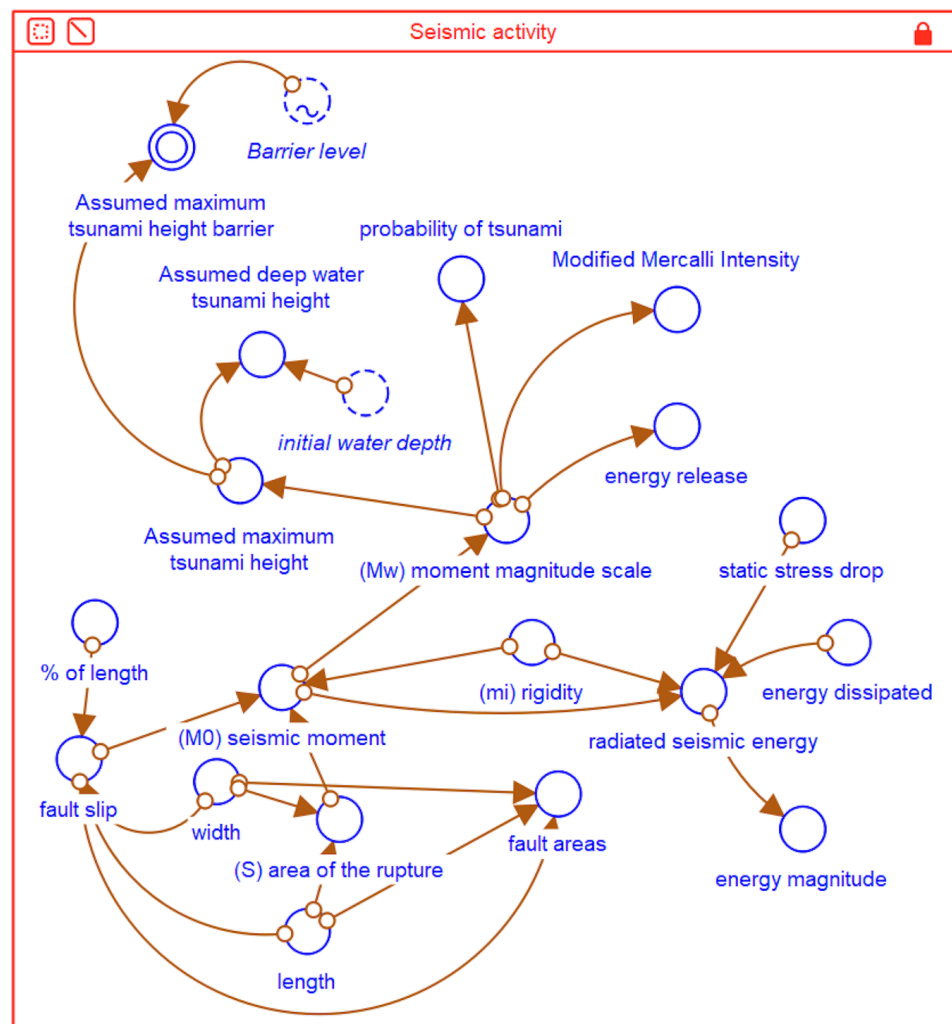
Apparently, it all starts with the formation of a tsunami. Developed links are arbitrary to enable meaningful and performable analysis. Together with the module containing defensive elements, the tsunami formation represents the “hard” part of the model in which exact relations among variables based on physical laws and principles must be modeled. Other modules contain more or less ambiguous relationships due to their softness. Their settings can be determined not only based on established relationships but also by model creators based on their expertise, best practices, or rules. The module contains tsunami formation and propagation and is presented in the following Figures 4 and 5.

This module is grounded in a set of converters, which mainly describe the behavior of the wave and their values. The module is based on equations presented in Appendix B. *Water depth* can be considered as the starting point of the module description. It is expressed using a graphical function. We have modeled a change in the depth of the water column, which is a function of time during the wave propagation and starts at the default value of 10,000 m and ends at 0 m. The change in the bottom terrain during the wave can be adjusted as needed based, for instance, on bathymetry data. Further variables associated with *water depth* are reckoned using the formulas from Appendix B.

The existence of *shallow water waves* must be verified, as tsunamis usually spread as this type of wave. This is verified by a simple condition that returns 0 if the shallow water wave does not exist and deactivates the module.

The *wave height* represents another important value associated with a wave at sea. Although unnecessary, the flow was chosen for this value instead of the converter, as this will allow a better connection with the *wave amplitude* value for which the conveyor must be used. The basic formula is used to determine the wave height at sea, which expresses that the more the sea depth decreases (the land approaches), the more the wave height increases. This value will be used to obtain information about the wave at the coast and the rise of the wave.

Another formula is based on maintaining wave energy flow and applies to so-called breaking and non-breaking waves. We also determine the value of the *run-up factor* and the *maximum run-up height*, which leads to the calculation of the *Imamura-Iida magnitude scale*. This scale includes twelve different grades based on seismic intensity [123]. Other values that the *maximum run-up height* needs as input are *wave height before shoaling* and *inclination of the coast*. Wave shoaling is an effect that causes the surface waves that enter the shore to change their height. The height of these waves is needed for the model. The value was set to 8 m for this particular wave. The inclination of the coast is also a given value of 1.30176852 radians.



(a)

Figure 4. Cont.

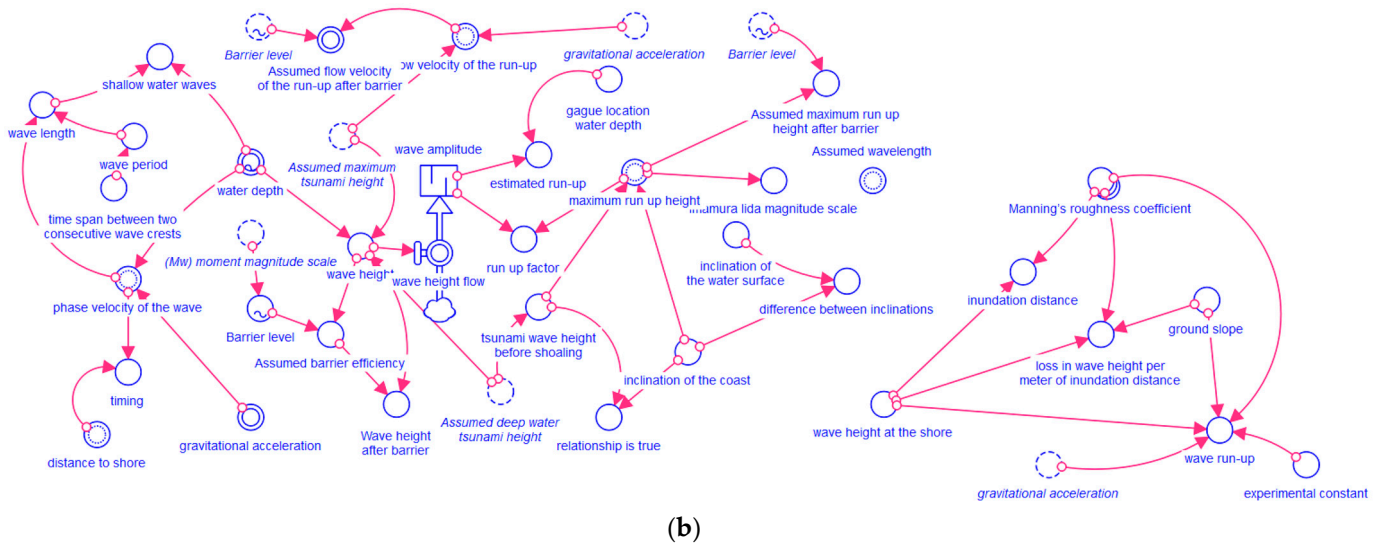


Figure 4. (a) Part of SD model: tsunami formation, seismic activity. Note: This part of the diagram shows the formation of a tsunami from seismic activity (own work; software: Stella Professional). (b) Part of SD model: tsunami formation. Note: This segment of the diagram focuses on wave formation. The area dealing with wave height shows that it is affected by water depth, wave amplitude, and wave propagation speed. The section dedicated to wave run-up illustrates how run-up is influenced by ground slope, surface roughness, and the loss in wave height per meter of inundation distance. The part of the diagram concerning waves behind a barrier includes factors like barrier level and barrier efficiency. This segment of the diagram focuses on tsunami simulation and includes parameters such as assumed water depth, assumed tsunami height, and wave distribution after propagating over various terrains (own work; software: Stella Professional).

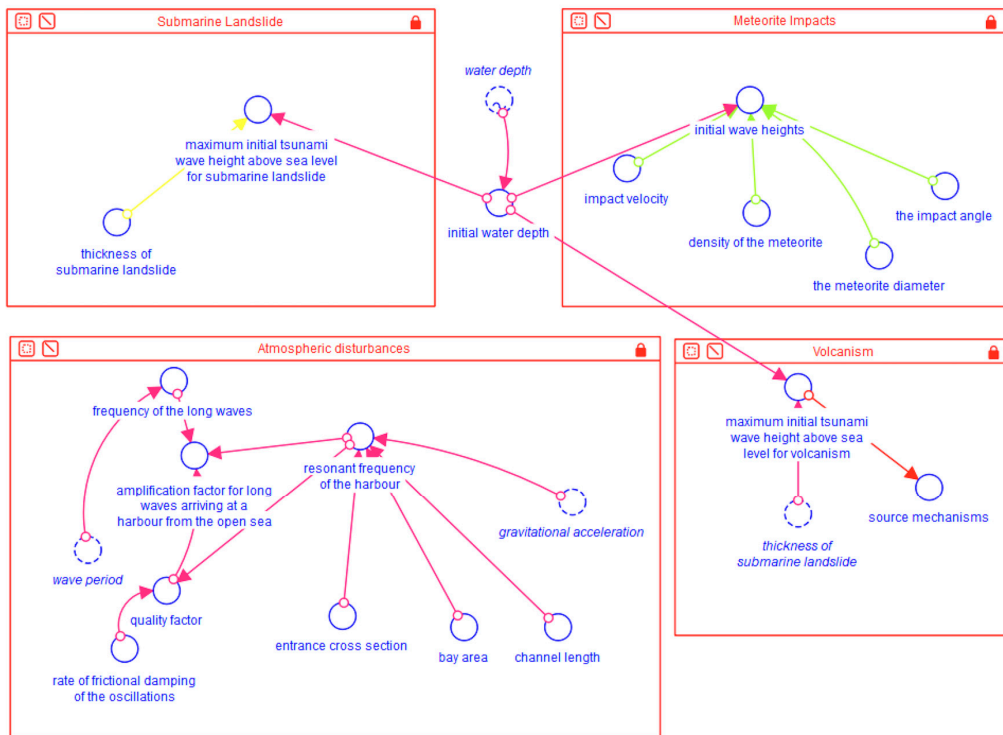


Figure 5. Part of SD model: tsunami formation, variants of formation. Note: This image shows diagram sections comprising other possible tsunami sources. Compared to Figure 4a, these are rather minor in terms of importance and frequency of occurrence (own work; software: Stella Professional).

The model uses another slope, namely the *Inclination of the water surface*. This is also set as a fixed value for the given wave as 0.00021025 radians. This value is then used to calculate the *flow velocity of the run-up*. We also need to calculate the value of inundation depth and the so-called Manning's roughness coefficient. The *Manning's roughness coefficient* is used in the Manning formula to calculate flow in open channels. In this case, the individual materials are entered in the fields, and a corresponding coefficient is added to them for easy material change. Now, for example, the material Earth Channel Weedy, a grassy earth channel with a coefficient of 0.030, is used [124]. This coefficient is also used for other calculations, such as *inundation distance* and flood distance. Its calculation uses only two values: coefficient and *wave height at the shore*, which is set at 1.928 m. *Wave height at the shore* is also used to calculate the *loss in wave height per meter of inundation distance* and the loss of wave height per meter of flooding distance. The last calculation is the wave run-up, which uses the above values and the so-called *experimental constant*, with a value of 0.5.

Five sectors further extend this basic module. These sectors deal with the emergence of the tsunami and can be linked to the primary model. Specific sectors are seismic activity, atmospheric disturbances, submarine landslides, meteorite impact, and volcanism.

3.2.2. People

This module illustrates the effect of a tsunami on the number of people in different categories, as presented in Figure 6. It is run entirely in units of People. Nine levels are included. In the first *Population in the state* reservoir, at time zero, the number of all people in the area affected by the tsunami is zero. In fact, except for the *Population in the state variable*, all other reservoirs are set to zero during the simulation initiation. This module is activated once the module *The formation of the Tsunami* is activated. The outflows separate the population into two other reservoirs, namely the affected population and the unaffected population, in both of these reservoirs at time zero because when the tsunami has not yet arrived, there is no need to distinguish between these two categories. People are further divided into those who are injured, dead, or uninjured into the *Injured people*, *Dead people*, and *Unharmed people* reservoirs. *Rescuers* is another reservoir where we have a number of rescuers in the area. Rescuers are then also divided into uninjured, wounded, and dead through model outflows. The last two reservoirs concern paramedics. The first is *Paramedics in the state*, where we have the number of all medics available, and the second is *Paramedics in the area*, where we have the number of all medics in a given location affected by the wave.

3.2.3. Buildings

This module, with the structure presented in Figure 7, demonstrates how the tsunami damaged or completely destroyed buildings in the area, as well as how reparation is funded from the *Finance* module later on. This module is influenced by *The formation of the Tsunami* module as well as the *Finance* module and is entirely in units of Buildings. The module is constructed based on the works of Leone et al. [125] and Rossetto et al. [126].

There are four reservoirs in this module, namely *Buildings*, *Damaged buildings*, *Repaired buildings*, and *Destructed buildings*. The Buildings repository contains a number of different types of buildings that are located in a given area. Buildings flow into the Damaged buildings storehouse, which are damaged by the tsunami and are classified according to the type of damage. Buildings that were completely destroyed by the tsunami wave flow into the Destructed buildings reservoir. After a while, the buildings will start to be repaired, and from the Damaged buildings reservoir, the buildings will start to flow into the Repaired buildings reservoir according to the volume of funds flowing from the last reservoir in this model, namely *Finances divided into areas*. This stock comes from the Finance module.

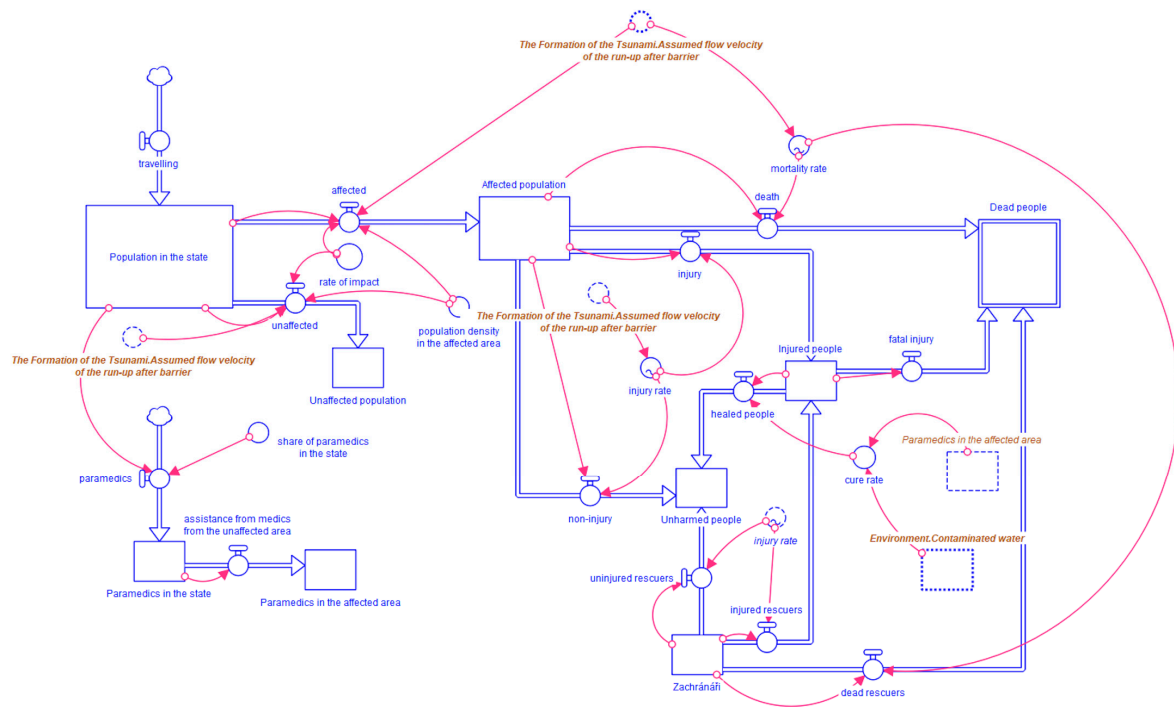


Figure 6. Part of SD model: impact on population. Note: This figure captures how the affected population is influenced by the impact rate and population density in the affected area. Mortality rate and injury rate determine the number of deaths and injured people, respectively. The diagram also includes the role of paramedics, showing how their assistance is divided between the unaffected and affected areas. Finally, the environment, specifically contaminated water, plays a role in the health outcomes of both injured people and rescuers, contributing to fatal injuries and deaths (own work; software: Stella Professional).

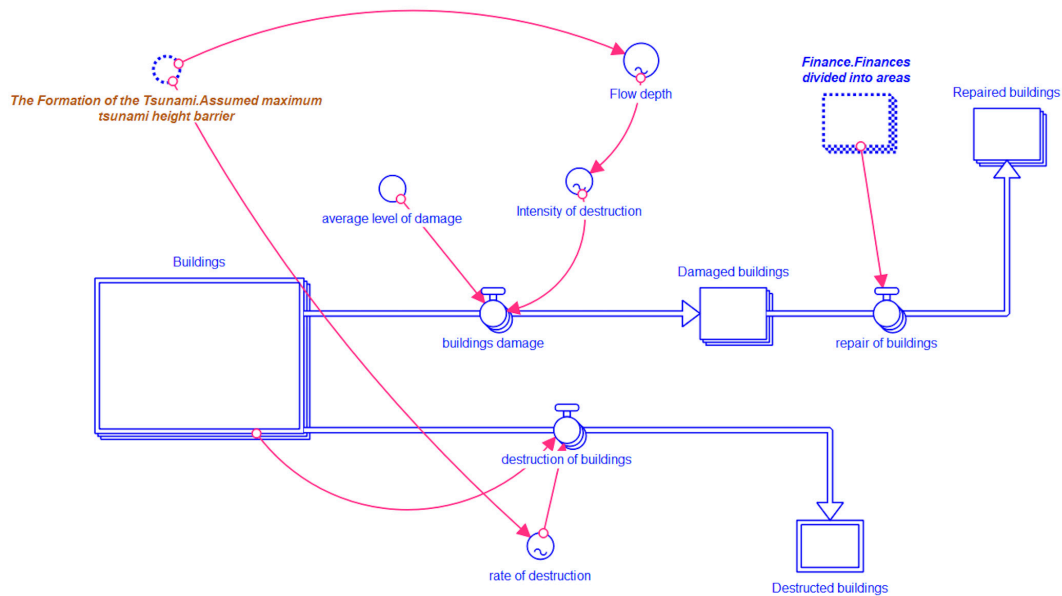


Figure 7. Part of SD model: impact on buildings. Note: This segment of the diagram focuses on the impact of a tsunami on buildings, specifically considering the assumed maximum tsunami height barrier. The flow depth and intensity of destruction affect the average level of damage to buildings. Damaged buildings are then categorized based on the rate of destruction (own work; software: Stella Professional).

In three reservoirs, *Buildings*, *Damaged buildings*, and *Repaired buildings*, we have used arrays, namely “Types of buildings”, where the buildings are divided according to their durability. In the *Damaged buildings* and *Repaired buildings* reservoirs, another array is used, namely “Damage”, where we have types of building damage (initial values are in oval brackets, array Damage has zero initial values):

- Array Types of building
- Wood and metal plates (180);
- Brick building (550);
- Larger reinforced brick buildings (90);
- Buildings with unreinforced concrete structures (63);
- Buildings with reinforced concrete structures (27).
- Array Damage
- Slight damage to the roof and furniture;
- Medium damage to walls and windows;
- Construction damage;
- Extreme construction damage.

3.2.4. Infrastructure

Based on the work of Ghobarah and Saatcioglu [127] and Valencia et al. [128], this module represents the damage of tsunamis to traffic communications (see Figure 8). Then, the wave damage to water pipes and poles with power cables is modeled here. The module also shows how communications and cable poles are repaired after the wave leaves with units of kilometers or meters. This module is influenced by the module *The formation of the Tsunami* and the *Finance* module.

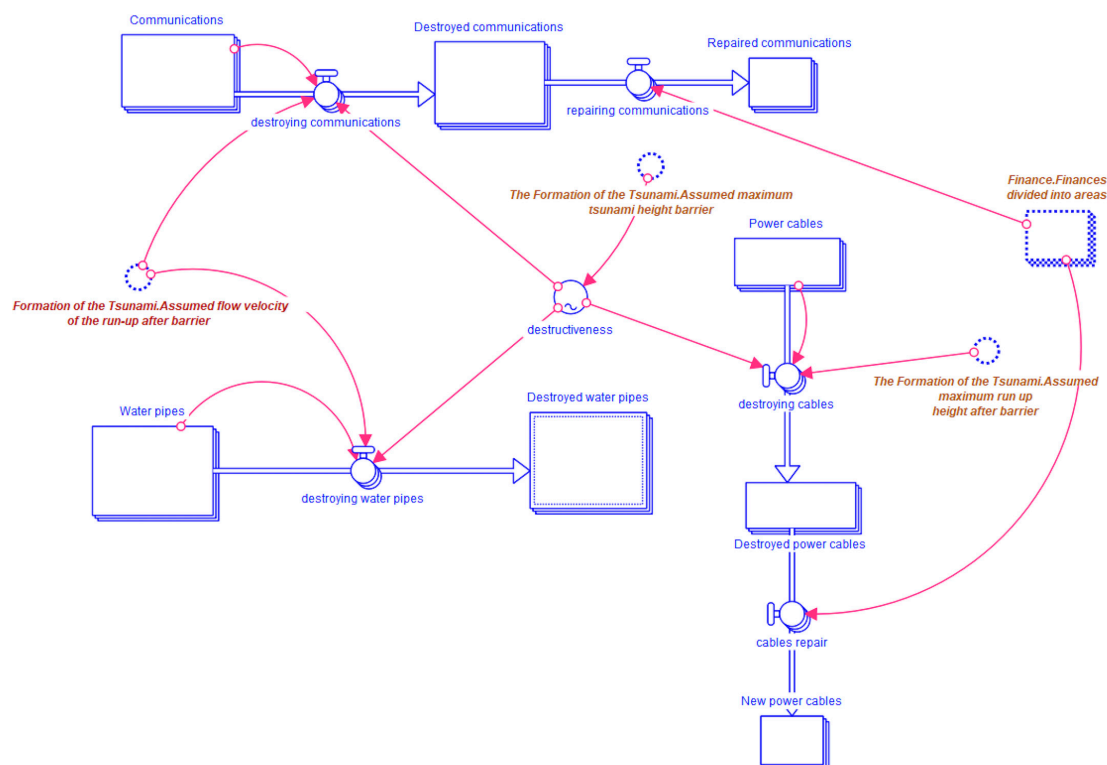


Figure 8. Part of SD model: impact on infrastructure. Note: This figure shows the infrastructure that a wave can damage or destroy. Several types of materials for each part can suffer from the tsunami impact. For example, water pipes can be plastic, copper, or steel (own work; software: Stella Professional).

There are three reservoirs in these modules: communications (Roads, Railways), water pipes (plastic, copper, metal), and power cables. Regarding communications, there are three repositories, namely *Communications*, *Destroyed communications*, and *Repaired communications* with units of kilometers. While initial values of Roads and Railways are set to 500 and 350, respectively, *Destroyed communications* and *Repaired communications* are set to 0 as the initial condition before the tsunami's arrival. Similar to communications, water pipes consist of water pipes and destroyed water pipes with an array applied to different types of pipes, namely plastic, copper, and metal. Initial values are set to 10,000, 20,000, and 15,000, respectively. *Destroyed water pipes* have the initial value set to 0. Power cables contain three stocks: *Power cables*, *Destroyed power cables*, and *New poles and cables*. A two-dimensional array is used here: Pole material and height. Materials considered are wood, concrete, and metal. Height is divided into groups lower than 5 m, from 5 to 10 m, and higher than 10 m. With respect to arrays, initial values are [30,000, 25,000, 15,000; 200,000, 15,000, 3000; 120,000, 30,000, 20,000]. Initial values of *Destroyed power cables* and *New power cables* are set to 0 again.

3.2.5. Finance

In this module, selected financial issues are modeled (see Figure 9). It demonstrates the amount of pledged financial resources and investments into the impacted area. Moreover, distribution to various areas is also included. The work of Heger and Neumayer [129] and Kweifio-Okai [130] is used to build particular model elements and relationships. There are three main modules interacting with Finance, namely Building, Environment, and People.

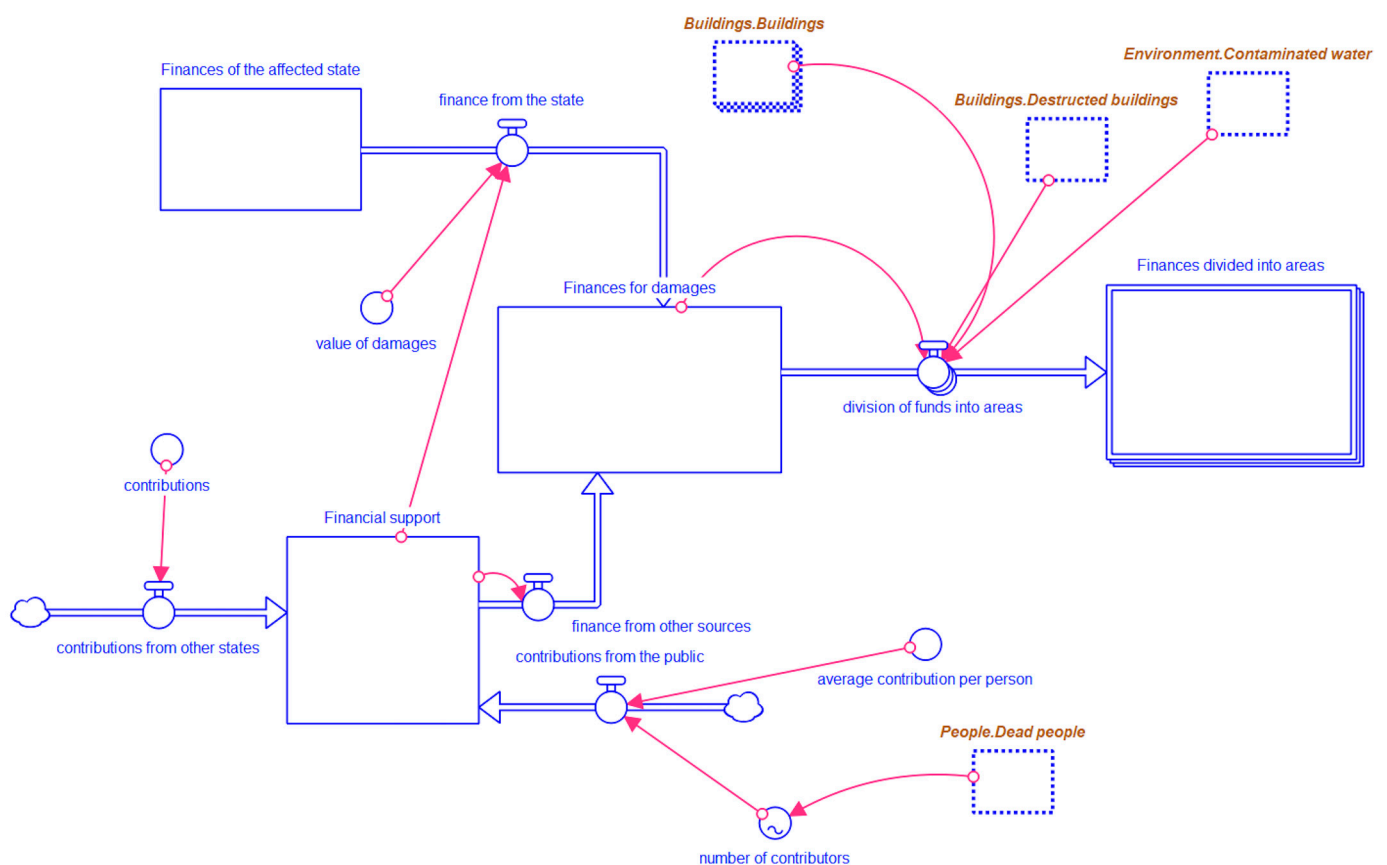


Figure 9. Part of SD model: financial impact. Note: This figure shows the financial aspect of the model, namely the income side. It considers state support and international financial aid, which usually comes with a delay (own work; software: Stella Professional).

This module has four reservoirs: Financial support, Finances of the affected state, Finance for damages, and Finance divided into areas. The first reservoir contains a value representing all the funds that have been raised to support the affected area from sources other than the state, such as contributions from other states, charities, or individuals. The second reservoir contains the finances of the affected state. Finances for damages add funds from the state and funds from other sources. The last reservoir contains an array of particular areas, which are Food, Infrastructure renewal, Water, Healthcare, Shelters, and Defense elements.

3.2.6. Defense Elements

The Defense element module consists of five sectors focusing on the most essential tools used in practice. All of these sectors overtake initial data from the module The formation of the Tsunami. This model is not directly linked to other modules. However, connection to other modules can be considered. For instance, an apparent connection can be made with the Finance module. Due to the illustrative nature of this model, further development in this direction is not applied. Although the modules are not interconnected, the financial side is also, at least, tentatively mentioned in the individual sections.

- **Self-elevating Seawalls**

Figure 10 presents the structure of the variables associated with self-elevating seawalls. Based on experiments and numerical analysis in OpenFOAM, the equations provided in Appendix C were used for calculations.

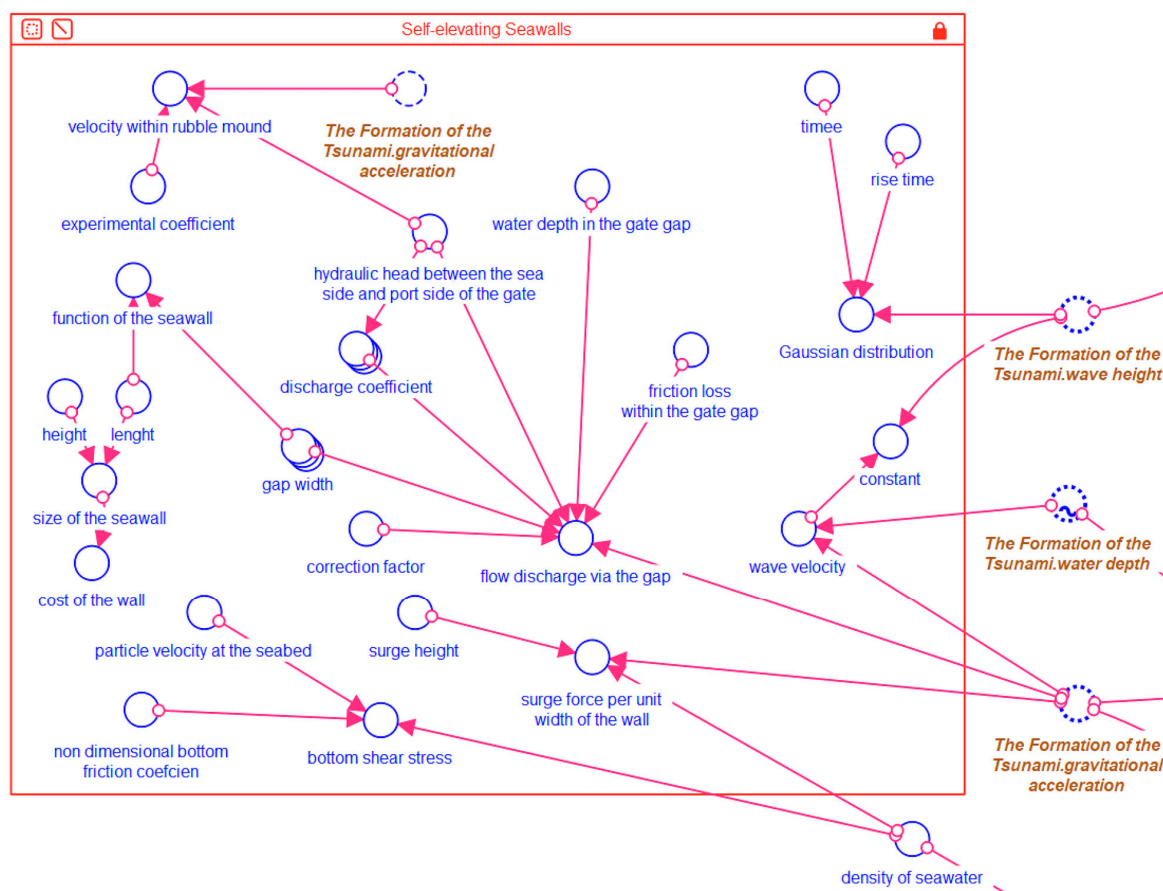


Figure 10. Part of SD model: self-elevating seawalls. Note: This figure exhibits the mechanism of self-elevating seawalls. This part of the model can be switched off as required. This option reflects the requirements of reality, where not every area can have this type of barrier (own work; software: Stella Professional).

The hydraulic head between the sea and the port side, where the gate is located, is represented in Equation 19 in Appendix C by the letter h , and this value is set at 2 m. The experimental coefficient value is set at 0.0354 to best determine the velocity in the so-called seepage flow, which is the flow of fluid (water) in the permeable layers, in our case, a rubble wall composed of stones with a diameter of 50 cm.

Next, *Surge force per unit width of the wall* is reckoned, while the density of seawater is $1.0273 \frac{\text{kg}}{\text{m}^3}$ and the surge height is 30 m. The time series of water levels could be represented by the Gaussian distribution, which can reproduce the rapid rise and subsequent fall of the water level η . Time is determined in seconds, and rise time indicates the time required to reach the top of the water level.

Flow discharge via the gap was calculated by taking advantage of Torricelli’s theorem. It is set as a condition because four different situations can occur, depending on the gap width and discharge coefficient setting, which must be lower than 1. The hydraulic head between the seaside and the port side of the gate is again represented by the letter h . The friction loss within the gate gap is set at 2 m. The water depth in the gate gap is set at 4.5 m. The last important value is the correction factor.

Friction loss within the gate gap can be calculated using the Darcy–Welsbach formula. This value should be small when the gate width is narrow. The condition below is based on Torricelli’s theorem. In any case, the discharge coefficient was derived purely from numerical analysis. Therefore, The correction factor aims to adjust the formula by incorporating other energy-dissipating mechanisms that cannot fully reproduce the hydrodynamic model Takagi et al. [131].

The discharge coefficient balances tsunami momentum and energy loss, leading to reduced flow, friction, shrinkage, expansion, and swirling. The larger the coefficient, the more momentum prevails, facilitating the flow of water through the gap. The regression between the discharge coefficient and the hydraulic head was derived for $w = 10, 15, 20, 30$ cm as follows.

$$w = 10 \text{ cm: IF}(h \leq 2)\text{THEN}((0.24 \times h) + 0.45) \text{ ELSE } 0.93 \tag{1}$$

$$w = 15 \text{ cm: } -0.04 \times h^2 + 0.34 h + 0.18 \tag{2}$$

$$w = 20 \text{ cm: } 0.15 h + 0.29 \tag{3}$$

$$w = 30 \text{ cm: } 0.15 h + 0.25 \tag{4}$$

The model sets the gap width and discharge coefficient as an array.

We can also determine whether the wall is functional or not based on the idea that the width of the gap in the floating breakwater system should be less than 3% of the total port breakwater section Nakashima et al. [132]. If applied condition 19 is met, the breakwater is functional. However, no technical procedure has been proposed to estimate the tsunami influx. The flow through such a constriction is usually complicated, so the resulting flow pattern is not easily subjected to any analytical solution.

The price is only estimated based on the Kamaishi Protection Breakwater in Japan, which is the deepest in the world. The price for $1 \text{ m}^2 = \text{USD } 8.954$ was determined and based on data from a hypothetical wall in a model for which we know the height, height, and length. So first, we calculate the size of the seawall $\text{size} = \text{height} \times \text{lenght}$. We can use the formula $\text{cost of the wall} = \text{size of the wall} \times 8.954$, for calculation of the cost of the wall, a hypothetical price in U.S. dollars.

- **Breakwaters**

The breakwaters sector, whose structure is presented in Figure 11, requires a wave height as an input value. Data for this particular model are taken from Ooya Harbor. Hudson’s formula [133,134] was used as a starting point during past tsunami events to analyze the stability of the defensive breakwater. According to this formula, the weight of the required armor is proportional to the wave height of the proposed incident. The density

of armor has a value of about $133 \times 1000 \text{ kg/m}^3$. In contrast, the relative underwater density of armor is only $15 \times 1000 \text{ kg/m}^3$. The slope of the structure was set to 30 rad for this situation. It should be noted that using the Empirically determined damage coefficient value is exposed to wind waves that do not exceed the peak for rubble structures. Therefore, the way the value is used here is not what it was intended for (i.e., for very long periods of waves exceeding rubble structures and breakwaters). Nevertheless, the armor units will benefit from the coupling effect when they resist the forces acting on them due to the tsunami currents. Without any better action, Esteban et al. [135] suggested that the Empirically determined damage coefficient values could be used, although it is clear that further research is needed on this issue.

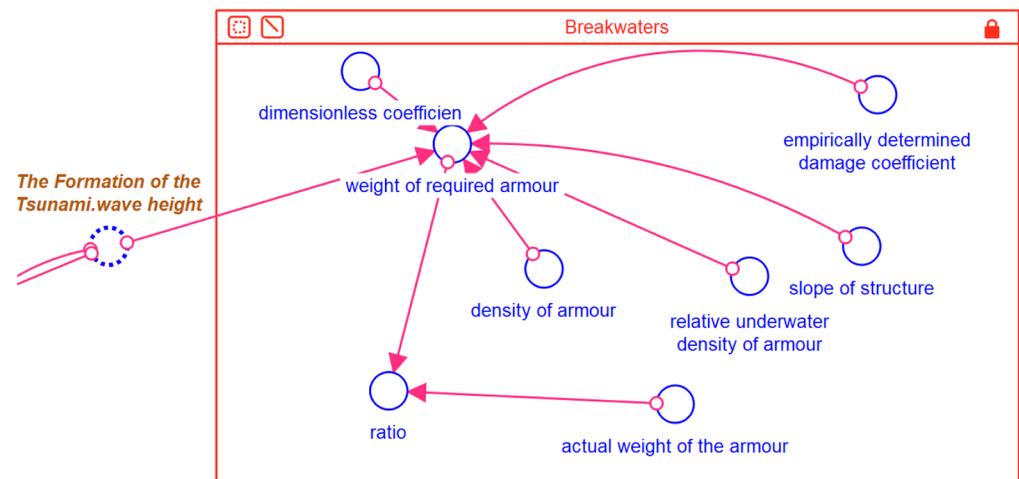


Figure 11. Part of SD model: breakwaters (own work; software: Stella Professional).

Unlike formulas such as Van der Meer [136], Hudson’s formula does not provide an indication of the degree of damage that can be expected as a result of an event. However, in order to quantify the strength of the structure, the armor damage was measured by a factor S similar to that used by Van der Meer. The ratio was defined as the ratio between the weight of the required armor and the actual weight of the armor.

- **Vertical deep barrier**

The vertical deep barrier sector with the structure presented in Figure 12 requires the input values water depth and gravitational acceleration. Pressure waves from earthquakes and landslides rebound from stable walls and then propagate back into the ocean [137]. High tsunamis develop only at depths of less than about 500 m or even 200 m. All calculations are based on the work of Levin and Nosov [138].

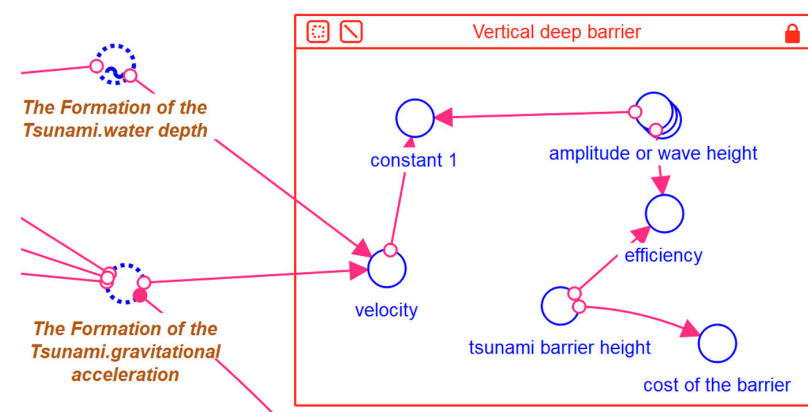


Figure 12. Part of SD model: vertical deep barrier (own work; software: Stella Professional).

An array is inserted in the amplitude or wave height for easy switching between sample values. We can also determine if the barrier is effective and efficient based on a simple condition $IF\ efficiency = (tsunami\ barrier\ height > amplitude\ or\ wave\ height)\ THEN\ 1\ ELSE\ 0$. We can also roughly determine the price based on the tsunami barrier height.

- **Other defense alternatives**

Two additional Defense elements were developed only for analytical purposes; their integration into the model is not necessary. These alternatives are the *Caisson breakwater* (see Figure 13) and the influence of coastal vegetation (see Figure 14).

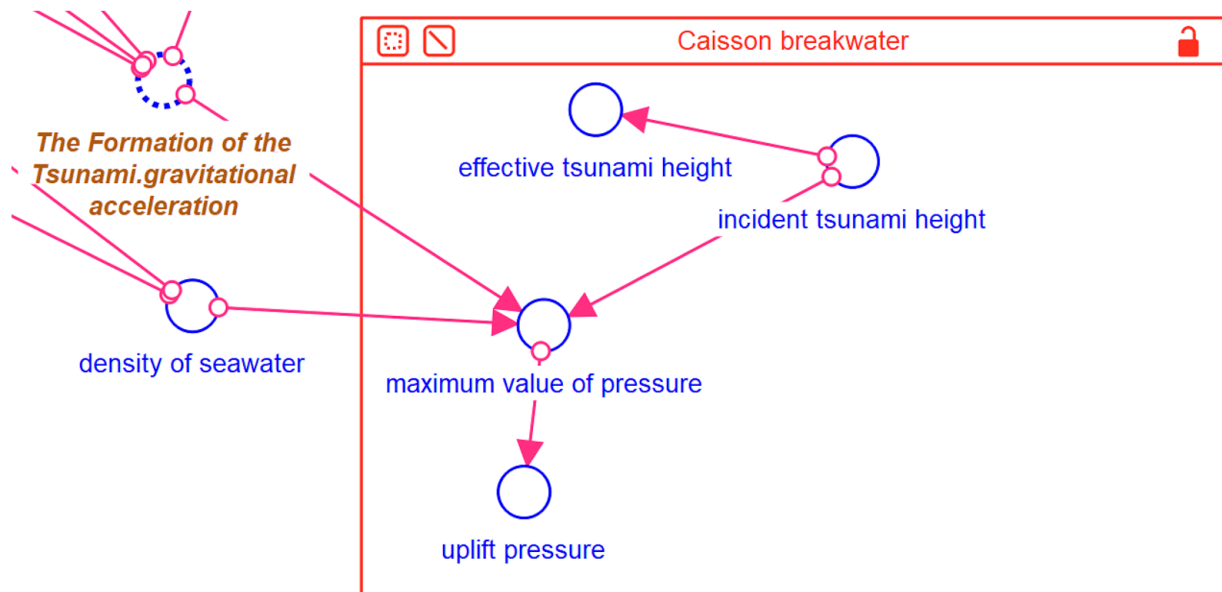


Figure 13. Part of SD model: Caisson breakwater (own work; software: Stella Professional).

3.2.7. Environment

This module shows how the tsunami will affect nature on the coast and at sea. There is also a model of drinking water contamination or sea pollution by various wastes. This module is affected by the module *The formation of the Tsunami*. This module (see Figure 15) is developed based on the work of Srinivas and Nakagawa [139].

There are four reservoirs in this module, namely Dead animals, Contaminated water, Destroyed coastal and sea life, and Waste in the sea. The values of all reservoirs are set to zero at the beginning of the simulation. The meanings of single reservoirs are self-explanatory. There are two arrays applied. In *Destroyed coastal and sea life*, types of vegetation, such as coral reefs, marine plants, mangrove forests, and coastal vegetation in cubic meters are used. In *Waste in the sea*, an array of specific types of waste is applied, namely (general) waste, soil, and debris. Waste is measured in kilograms and indicates the number of different types of waste that enter the sea when the wave recedes.

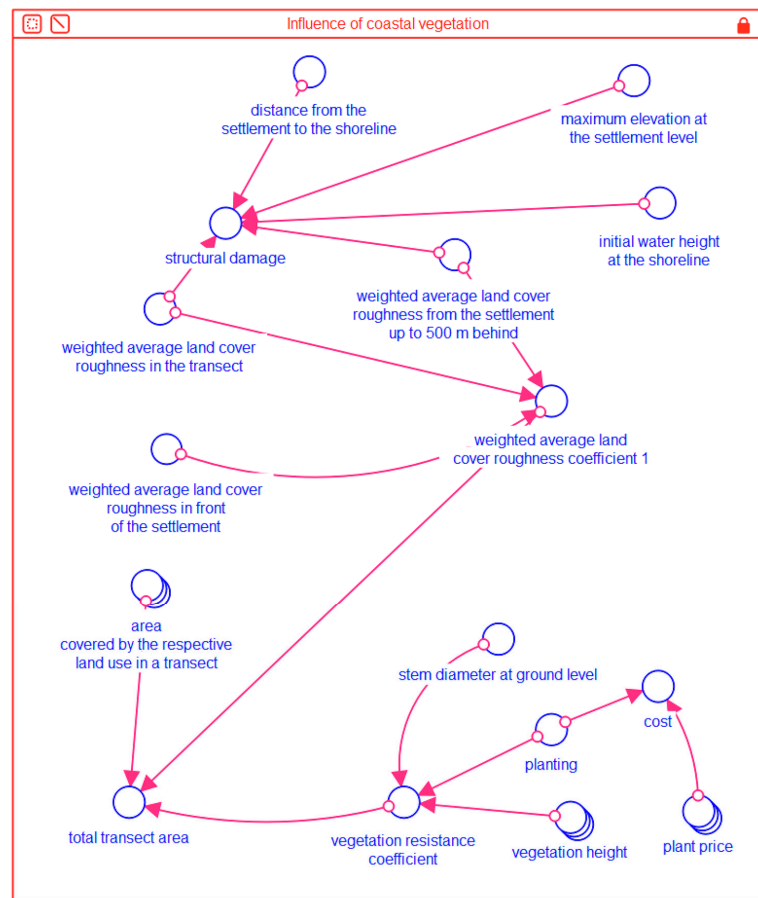


Figure 14. Part of SD model: influence of coastal vegetation. Note: This figure shows the impact of the wave on the vegetation and vice versa. There are several types of vegetation in this part of the model, and different vegetation parameters are assumed (own work; software: Stella Professional).

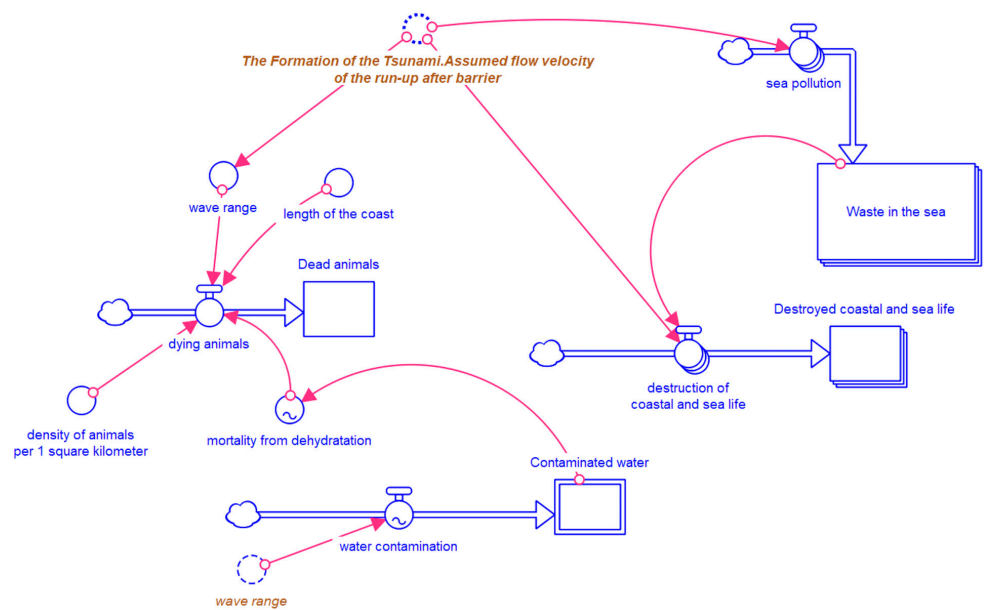


Figure 15. Part of SD model: impact on fauna and flora. Note: This part of the model shows the impact of the wave on fauna and flora. The amount of waste moved into the sea and the amount of marine life destroyed are examples of the main indicators monitored here (own work; software: Stella Professional).

3.2.8. Model Simulation

Due to the main purpose of the model and its illustrative nature, simulations were not used for the analysis or for finding a solution for a specific case or event. The aim was to show the possibilities of system dynamics in connecting various disciplines into one multidisciplinary descriptive mechanism. Therefore, all tests usually executed on the available model, such as what-if or sensitivity analysis, were not conducted. However, the model successfully passed the robustness test under extreme conditions and structural and behavioral tests.

The initial model parametrization is based on values indicated in previous sections presenting particular modules and sectors. Further parametrization is based on data associated with a specific tsunami wave from 2004 in the Banda Aceh area of Indonesia. Further settings can be found in the model, which is included in the Appendices A–C associated with this manuscript. There is one principal issue associated with the simulation. The model contains processes that take place in various time units. Simple unification is not possible in one model. We can either develop two separate models based on specific time units or use multiple simulations with simultaneous switching off of selected sectors. However, the solution is feasible. The one-hour step was selected as the time unit for the simulations used for all modules except the Formation of tsunami and Defense elements. These two modules use the one-second step. The following figures demonstrate the dynamics of the selected variable in each module. Figure 16 shows the situation of the population 100 h after the start of the simulation. The population was first divided into affected and unaffected populations. The affected population became either injured, uninjured, or dead. Figure 17 shows the size of the destruction in terms of communications and water pipe damage. As determined by the model’s initial parametrization, roads are being repaired in terms tens of hours while the reparation of water pipes is postponed. Figures 18 and 19 present the outputs of the sensitivity analysis. Figure 18 captures the barrier utility at different levels of barrier effectiveness and different levels of potential wave height at impact. The right part of the graph (shown in green and separated by the black line) captures usefulness greater than 91%. The black line (on the right side) defines the region of usefulness between 89% and 91%. The part of the graph between the black lines describes the condition where the barrier application is useful. The left part of the graph (to the left black line) shows the situation where the application of the barrier is counterproductive. Figure 19 captures the change in the utility of barrier application relative to the effectiveness of the barrier and the potential wave height.

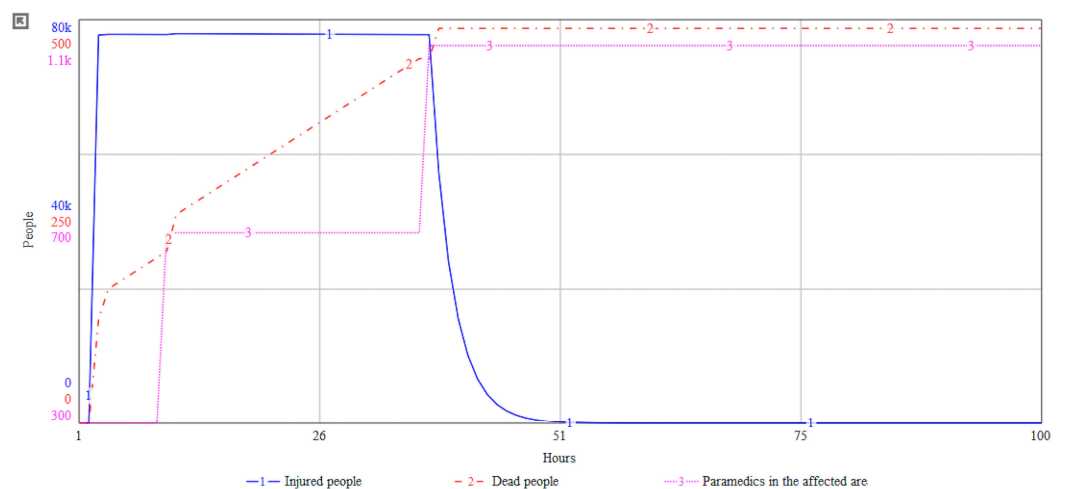


Figure 16. Temporal dynamics of casualties and emergency response following a tsunami. Note: The vertical axis is monitored in units of People; all three variables can reach values between predefined minima and maxima (Injured people min = 0, max = 80,000; Dead people min = 0, max = 500; Paramedics in the affected area min = 300, max = 1100) (own work; software: Stella Professional).

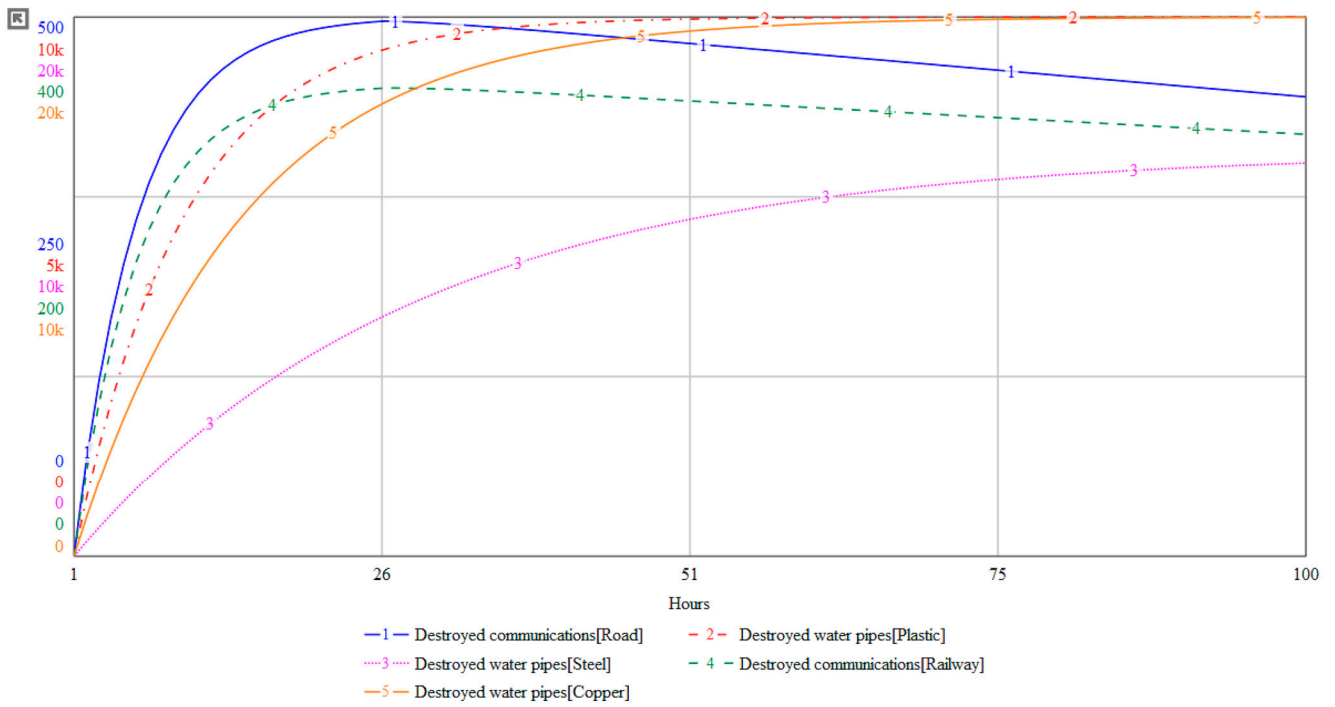


Figure 17. Infrastructure damage assessment over time after tsunami impact. Note: Monitor variables have predefined maximal values (Destroyed roads max = 500, Destroyed plastic water pipes max = 10,000, Destroyed steel water pipes max = 20,000, Destroyed railways max = 400, Destroyed copper water pipes max = 20,000) (own work; software: Stella Professional).

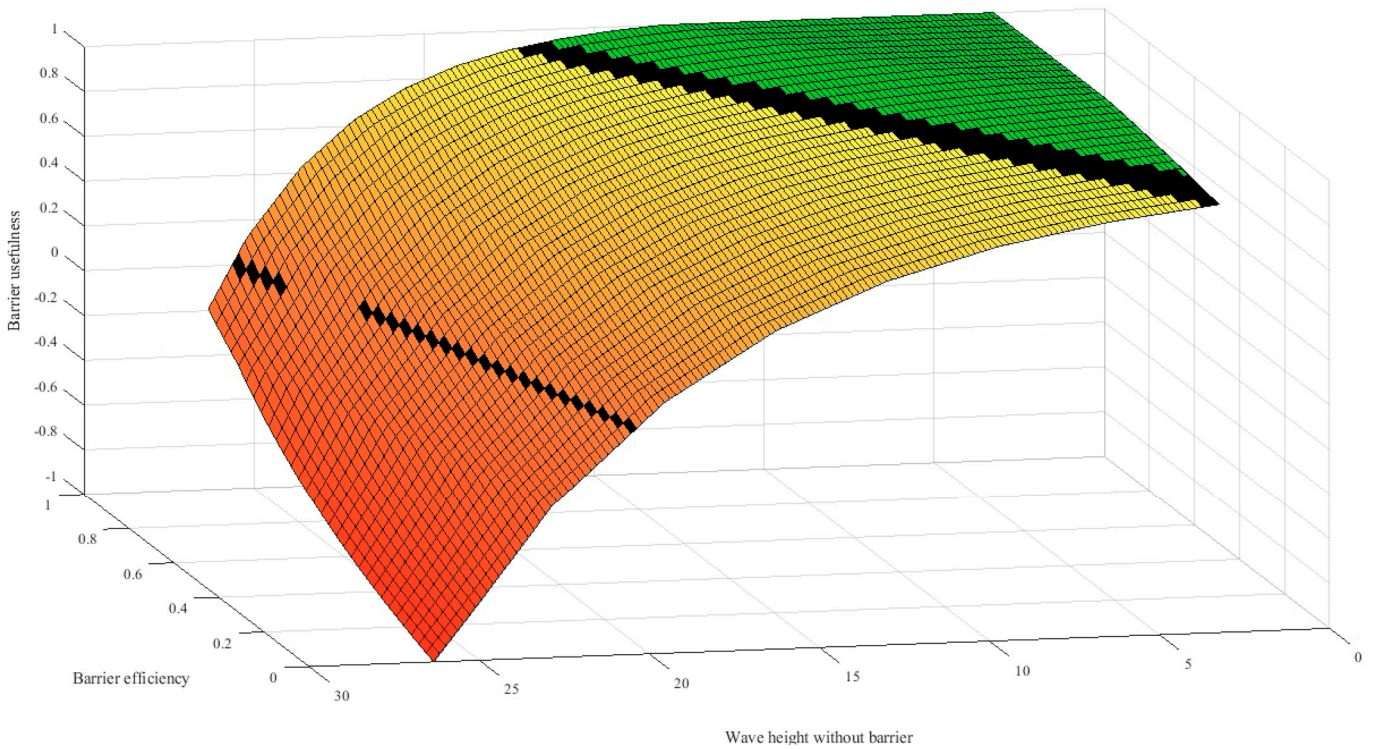


Figure 18. Simulation of barrier effectiveness in wave height reduction (own work; software: MatLab).

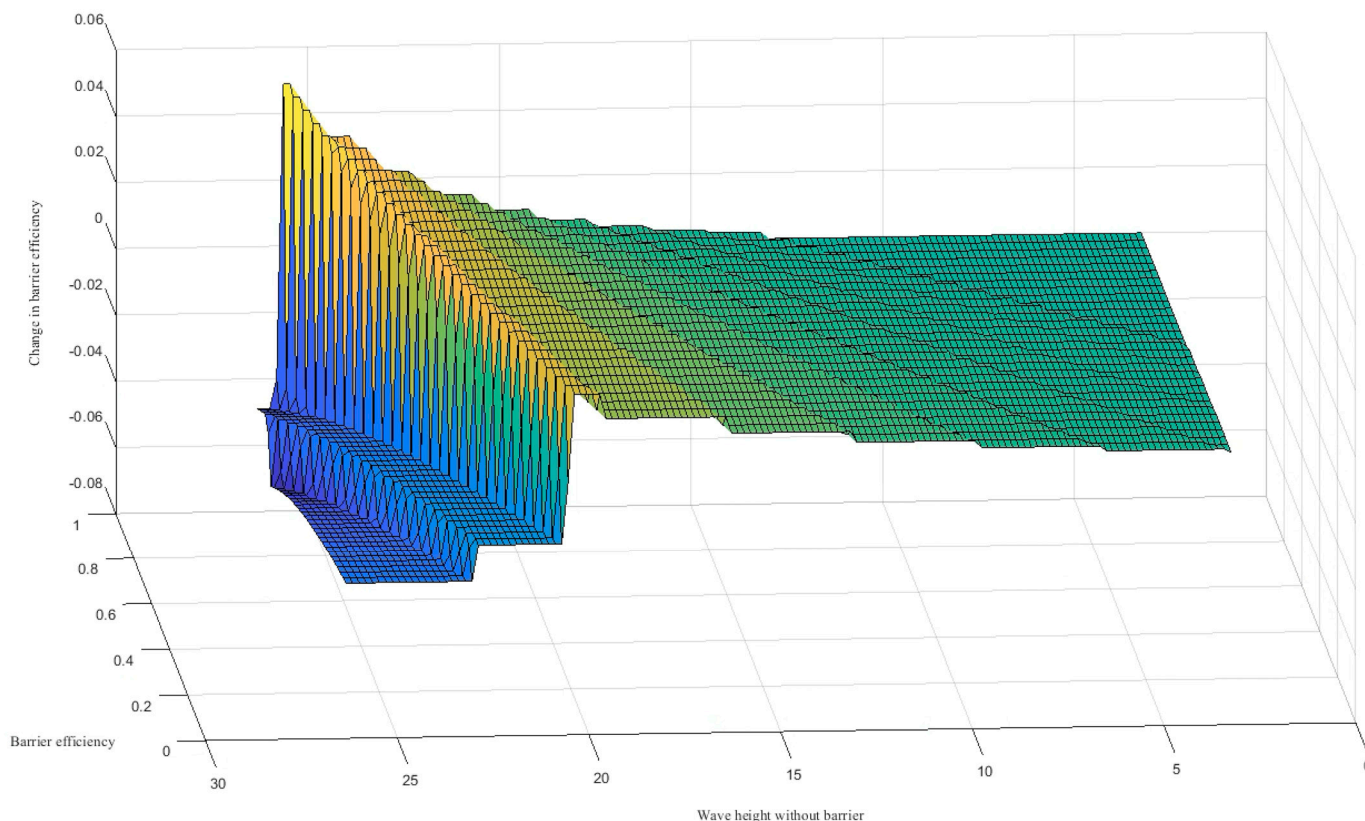


Figure 19. Impact of barrier efficiency on wave height attenuation (own work; software: MatLab).

4. Study Limitations

This study has several principal limitations, which can be clustered into two segments. The first segment contains issues related to the literature review and analysis that was conducted. The second one is associated with the developed model. As for the former, the first limitation is the incomplete identification of all relevant articles. We were not able to circumvent this limitation because of the use of the term “tsunami” even in a field where it is used in a context other than its original meaning, an example being “obesity tsunami” or “addiction tsunami”, etc. Based on the use of this word, we had to add an auxiliary relevant keyword to remove redundant articles. This step may have caused not all relevant articles to be found. Another limitation is in the search for software used, where not all studies mention the name of the software used and/or do not use the word “software” next to the software name. We were able to partially circumvent this limitation by using a double-machine full-text search, wherein the first step, the retrieved articles were searched for the term “software”, followed by recording the names of the reported software and then performing a full-text search for the names of the retrieved software. Another limitation was that not all articles were found in the full-text version. Additional steps may be taken in future replications or extensions of this study to obtain a comprehensive pool of articles. Moreover, additional resources and paper repositories are available. Searching their content, on the other hand, would result in more redundancy in acquired papers rather than new discoveries. Regarding the model itself, we need to highlight that the purpose of the presented model is to demonstrate the possibility of integrating various disciplines in the investigation of complex multidisciplinary phenomena. Thus, particular modules and subsystems may seem to be incomplete or need to be elaborated. Indeed, they are, and they do need. The main intention is to outline how tsunami research can be at least partially consolidated. Elaboration would lead to a higher density of interconnections, which does not have to support comprehensibility and meaningfulness. Although the presented study is comprehensive, the list of tools, techniques, methods, or software

toolkits cannot be fully exhausted. Various software applications are used for particular and specific aspects of tsunami-related science [140]. For instance, the topic of the fragility of constructions due to the tsunami impact (e.g., [141–148]) can serve as an example, which is not explored much in this study. However, the goal of this paper was not to create a comprehensive picture of tsunami research but only the part where tsunami-related software and modeling methods are used to investigate tsunamis. In future research, we could compare approaches to tsunami research using software and “software-free” tsunami research. The most significant challenge is related to the time units used in the model. There are processes that are more convenient to simulate in seconds or minutes, while other processes take place in the order of hours or days. Unification in the system dynamics model can be achieved, for instance, by developing the simulation of two separate models. This represents the main research challenge in this domain.

5. Conclusions

With advances in computing power and software for modeling and simulation, the capabilities in the vast majority of scientific fields have advanced [149], and this is also true in the field of tsunami research [150]. In our study, we identified the most widely used software and methods in the tsunami field over the last decade. We also identified the sectors in the tsunami field where software and methods are used. Furthermore, we have assigned each software and method their function for the analyzed article. The most significant software packages in the tsunami research we identified include OpenFOAM, CALIB, MATLAB, ArcGIS, and COMCOT. The methods we have identified belong to various fields of study and are mostly focused on the tsunami origin or its propagation, exploring historical tsunamis based on tsunami deposits, modeling tsunamis in 3D space, identifying tsunami impacts, exploring relevant variables for tsunamis, creating tsunami impact maps, and comparing simulation results with real data. Various methods are applied, such as the Accelerator Mass Spectrometry, Computational Fluid Dynamics, Constant Rate of Supply Method, Digital Elevation Models, Finite Area Method, Fuzzy C-Means Clustering, and probabilistic tsunami hazard analysis. The importance of finding a tool that would not be over-specialized and narrowly focused on particular aspects of tsunamis needs to be emphasized as the main added value of this study. It is apparent that the existing specialized tools or methods used in particular fields of study need to be applied to find answers to particular domain-related research questions. However, due to the multidisciplinary nature of tsunamis, the more complex systems approach needs to be applied. The holistic view and feedback structures with mutually interconnected parts represent its primary attributes. Data or information acquired by tools, techniques, or modeling software can be used as inputs to more complex models, which would improve understanding and insights into tsunami phenomena. No study used or mentioned the possibility of applying system dynamics as a methodological tool, which focuses on capturing change and behavior over time. This approach is applied in various disciplines. This study demonstrates that the application of system dynamics as a commonly used modeling and simulation methodology can be successfully used for the implementation of the system perspective in tsunami research.

Author Contributions: Conceptualization, M.Z. and V.B.; methodology, V.B., D.P. and P.Č.; software, M.Z., T.N. and M.H.; validation, S.I., P.M. and B.E.S.; formal analysis, B.N.A.; investigation, M.Z., B.N.A., T.N. and D.P.; resources, F.B. and S.I.; data curation, F.B.; writing—original draft preparation, M.Z., V.B., T.N., P.Č. and M.H.; writing—review and editing, B.E.S., P.M. and S.I.; visualization, M.Z.; supervision, V.B.; project administration, V.B.; funding acquisition, V.B. and P.M. All authors have read and agreed to the published version of the manuscript.

Funding: This research received no external funding.

Institutional Review Board Statement: Not applicable.

Informed Consent Statement: Not applicable.

Data Availability Statement: The data presented in this study are available on request from the corresponding author.

Acknowledgments: The VES20 Inter-Cost LTC 2020 project supported this research. The authors also express gratitude to the COST Action AGITHAR leaders and team members. The Faculty of Informatics and Management UHK Specific research project “Addressing modern research topics with increased student involvement” has also partially supported the research. The authors thank Patrik Urbanik and Jan Boura for their assistance.

Conflicts of Interest: The authors declare no conflicts of interest.

Appendix A

Table A1. SW tools description.

Tool	Website	Usage	In Total
Agisoft	https://www.agisoft.com/ , accessed on 15 March 2023	For photogrammetric process; for image post-processing	3
Agisoft Metashape is a stand-alone software product that performs photogrammetric processing of digital images and generates 3D spatial data to be used in GIS applications, cultural heritage documentation, and visual effects production, as well as for indirect measurements of objects of various scales.			
Amira	https://www.thermofisher.com/cz/en/home/electron-microscopy/products/software-em-3d-vis/amira-software.html , accessed on 15 March 2023	Tsunami waves visualization	1
Amira Software is a comprehensive and versatile 2D–5D solution for visualizing, analyzing, and understanding life science and biomedical research data from many image modalities, including Optical and Electron Microscopy, CT, MRI, and other imaging techniques. With incredible speed and flexibility, Amira Software supports advanced 2D–5D bioimaging workflows in research areas ranging from structural and cellular biology to tissue imaging, neuroscience, preclinical imaging, and bioengineering. From any 3D image data, including time series and multi-channel, Amira Software delivers a comprehensive range of data visualization, processing, and analysis capabilities. Amira Software allows life science and biomedical researchers to gain invaluable insights into their data at different scales and from any modality.			
ANSYS	https://www.ansys.com/ , accessed on 15 March 2023	Modeling and validation of numerical models; to build numerical model; to build a channel domain	5
Ansys Discovery is the first simulation-driven design tool to combine instant physics simulation, proven Ansys high-fidelity simulation, and interactive geometry modeling in a single user experience.			
ArcGIS	https://www.ArcGIS.com/index.html , accessed on 15 March 2023	To identify blocks; for merging and checking data; for calculation of slope gradient; for evacuation potential; to plot a tectonic map; to subtract backscatter and seismic data, the post-slide bathymetry grid; to create map of studied area; for incorporating collected data; to model wave heights and inundation for a range of SLR scenarios	15
ArcGIS offers unique capabilities and flexible licensing for applying location-based analytics to your business practices. Gain greater insights using contextual tools to visualize and analyze your data. Collaborate and share via maps, apps, dashboards, and reports.			
CALIB	http://calib.org/calib/ , accessed on 15 March 2023	To calibrate radiocarbon ages	12
Without official description			
COMCOT	https://citeseerx.ist.psu.edu/viewdoc/download?doi=10.1.1.512.84&rep=rep1&type=pdf , accessed on 15 March 2023 Note: We could not find official website; included link is to manual for COMCOT software	NSWE solver; to simulate the entire life-span of a tsunami; to simulate tsunami propagation from its origin to coastal areas; to simulate tsunami events; for the wave propagation; to validate combination of time step, grid spacing, and depth	9
COMCOT (Cornell Multi-grid Coupled Tsunami model) adopts explicit staggered leap-frog finite difference schemes to solve Shallow Water Equations in both Spherical and Cartesian Coordinates. A nested grid system, dynamically coupled up to 12 levels (which will also be referred to as layers) with different grid resolutions, can be implemented in the model to fulfill the need for tsunami simulations in different scales.			
Delft3D	https://oss.deltares.nl/web/delft3d , accessed on 15 March 2023	To create a grid; to simulate tsunami; to model wave heights and inundation for a range of SLR scenarios	4
Delft3D is open-source software and facilitates the hydrodynamic (Delft3D-FLOW module), morphodynamic (Delft3D-MOR module), waves (Delft3D-WAVE module), water quality (Delft3D-WAQ module including the DELWAQ kernel), and particle (Delft3D-PART module) modeling.			
DSAS	https://www.usgs.gov/centers/whcm/science/digital-shoreline-analysis-system-dsas?qt-science_center_objects=0#qt-science_center_objects , accessed on 15 March 2023	Determination of coastline change	1
The Digital Shoreline Analysis System (DSAS) v5.0 software is an add-in to Esri ArcGIS desktop 10.4–10.6 that enables a user to calculate rate-of-change statistics from multiple historical shoreline positions. It provides an automated method for establishing measurement locations, performs rate calculations, provides the statistical data necessary to assess the robustness of the rates, and includes a beta model of shoreline forecasting with the option to generate 10- and/or 20-year shoreline horizons and uncertainty bands.			
Fledermaus	https://qps.nl/fledermaus/ , accessed on 15 March 2023	For digital elevation models	1
Fledermaus unlocks the potential of data, with a wide variety of analysis tools working in 3D or 4D space. With fast and easy presentation tools, it shows data better than ever before.			
FLOW3D	https://www.flow3d.com/ , accessed on 15 March 2023	Simulate tsunami	1
FLOW-3D is an accurate, fast, proven CFD software that solves the toughest free-surface flow problems. A pioneer in the CFD industry and a trusted leader, FLOW-3D is a highly efficient, comprehensive solution for free-surface flow problems with human-centric support.			
Gambit	http://geoweb.mit.edu/gg/ , accessed on 15 March 2023	To generate geometry and meshes of the numerical model	1

Table A1. *Cont.*

Tool	Website	Usage	In Total
<p>GAMIT, GLOBK, and TRACK form a comprehensive suite of programs for analyzing GNSS measurements primarily to study crustal deformation. The software has been developed by MIT, Scripps Institution of Oceanography, and Harvard University with support from the National Science Foundation. The software may be obtained without written agreement or royalty fee by universities and government agencies for any non-commercial purposes.</p>			
GeoClaw	http://www.clawpack.org/geoclaw , accessed on 15 March 2023	To model tsunami; to simulate tsunami	5
<p>It is a variant of Clawpack for geophysical flows. Clawpack is a collection of finite volume methods for linear and nonlinear hyperbolic systems of conservation laws. Clawpack employs high-resolution Godunov-type methods with limiters in a general framework applicable to many kinds of waves. Clawpack is written in Fortran and Python.</p>			
Geosoft Oasis	https://www.seequent.com/products-solutions/geosoft-oasis-montaj/ , accessed on 15 March 2023	To create color surface plot from simulation results	1
<p>QA/QC, transform, and analyze all raw data—geology, geochemistry, and geophysics—with powerful 2D and 3D modeling capabilities.</p>			
Geowave	https://www.osgeo.org/projects/geowave/ , accessed on 15 March 2023	To generate tsunami and wave propagation	1
<p>GeoWave is a software library that connects the scalability of distributed computing frameworks and key-value stores with modern geospatial software to store, retrieve, and analyze massive geospatial datasets.</p>			
HAZUS	https://www.fema.gov/flood-maps/products-tools/hazus , accessed on 15 March 2023	To define building damage states	1
<p>FEMA’s Hazus Program provides standardized tools and data for estimating risk from earthquakes, floods, tsunamis, and hurricanes. Hazus models combine expertise from many disciplines to create actionable risk information that increases community resilience. Hazus software is distributed as a GIS-based desktop application with a growing collection of simplified open-source tools. Risk assessment resources from the Hazus program are always freely available and transparently developed.</p>			
HydroSed2D	https://sourceforge.net/projects/hydroSed2d/ , accessed on 15 March 2023	To investigate tsunami wave run-up and land inundation on coastal beaches	1
<p>HydroSed2D is a two-dimensional numerical model for hydrodynamics and sediment transport on unstructured mesh.</p>			
ICEM	https://www.3ds.com/products-services/catia/products/icem-surf/ , accessed on 15 March 2023	Mesh generation	1
<p>ICEM Surf is the industry-leading Curve and Surface explicit geometry modeling tool for defining, analyzing, and performing high-end visualization of complex free-form shape CAD surface models to the highest quality. Used in product design processes throughout automotive, aerospace, consumer goods, and press-tool design industries, providing solutions for direct surface modeling, refinement, reconstruction, and scan modeling.</p>			
MATLAB	https://www.mathworks.com/products/matlab.html , accessed on 15 March 2023	To solve the eigenvalue problem; to compare results and estimate; to compute wind-driven flow; to classify pre- and post-tsunami images; to simulate time steps; to export and reformat grid; to perform gradient-based optimization algorithm; to process data; to solve part of the system	15
<p>MATLAB® combines a desktop environment tuned for iterative analysis and design processes with a programming language that expresses matrix and array mathematics directly. It includes the Live Editor for creating scripts that combine code, output, and formatted text in an executable notebook.</p>			
MB-System	https://www.mbari.org/products/research-software/mb-system/ , accessed on 15 March 2023	To calculate seafloor attributes; to generate the one-ninth arc-second coastal DEM	2
<p>MB-System is an open-source software package for the processing and display of bathymetry and backscatter imagery data derived from multibeam, interferometry, and sidescan sonars.</p>			
OpenFOAM	https://www.openfoam.com/ , accessed on 15 March 2023	To develop a nonlinear three-dimensional coupled model; to create 3D model; to use its solver; to calculate the flow field under the water surface; to create model of 3D numerical wave tank; to create model of tsunami barriers and tsunami impacts; to create a hydrodynamic and morphologic model; to create tsunami model; to simulate tsunami; to calculate properties of tsunami	25
<p>OpenFOAM is the free, open-source CFD software developed primarily by OpenCFD Ltd. since 2004. It has a large user base across most areas of engineering and science, from both commercial and academic organizations. OpenFOAM has an extensive range of features to solve anything from complex fluid flows involving chemical reactions, turbulence, and heat transfer to acoustics, solid mechanics, and electromagnetics.</p>			
OsiriX DICOM	https://www.osirix-viewer.com/ , accessed on 15 March 2023	To construct a 3D image of stones and to measure its dimensions, volume, and surface area	1
<p>It fully supports the DICOM standard for easy integration in your workflow environment and an open platform for the development of processing tools. It offers advanced post-processing techniques in 2D and 3D, exclusive innovative techniques for 3D and 4D navigation, and a complete integration with any PACS.</p>			
QGIS	https://qgis.org/en/site/ , accessed on 15 March 2023	To create a map; to generate mesh	3
<p>QGIS is a professional GIS application that is built on top of and proud to be itself Free and Open-Source Software (FOSS).</p>			
R-studio	https://www.rstudio.com/ , accessed on 15 March 2023	To calibrate ages of tsunami deposits	1
<p>RStudio’s mission is to create free and open-source software for data science, scientific research, and technical communication. We do this to enhance the production and consumption of knowledge by everyone, regardless of economic means, and to facilitate collaboration and reproducible research, both of which are critical to the integrity and efficacy of work in science, education, government, and industry.</p>			
reflexW	https://www.sandmeier-geo.de/reflexw.html , accessed on 15 March 2023	To process Ground-Penetrating Radar data	1
<p>he software covers the complete range of wave data (seismic, GPR, ultrasound) and the different geometry assemblings (surface reflection and refraction, borehole crosshole and tomography, and combination of borehole and surface measurements). You may also have a look at a one-sided brochure for GPR, reflections seismics, refraction seismics, and borehole application.</p>			
SPAD	https://ia-data-analytics.com/data-mining-software/ , accessed on 15 March 2023	To apply statistical test on data	1

Table A1. *Cont.*

Tool	Website	Usage	In Total
Coheris Analytics SPAD is the only software dedicated to Data Mining and Predictive analysis that provides a totally graphical and intuitive interface with powerful features.			
tsunami-2d	https://www.ornl.gov/team/scale/sensitivity-and-uncertainty-analysis-0 , accessed on 15 March 2023	To apply sensitivity analysis and propagation of uncertainties of cross-sections; to conduct sensitivity and uncertainty analysis	2
The TSUNAMI-1D, TSUNAMI-2D, and TSUNAMI-3D analysis sequences compute the sensitivity of keff and reaction rates to energy-dependent cross-section data for each reaction of each nuclide in a system model. The one-dimensional (1D) transport calculations are performed with XSDRNP, the two-dimensional (2D) transport calculations are performed using NEWT, and the three-dimensional (3D) calculations are performed with KENO V.a or KENO-VI.			
VOLNA	https://gmd.copernicus.org/articles/11/4621/2018/ , accessed on 15 March 2023	To compare results with presented numerical solver; to simulate tsunami	2
A finite-volume nonlinear shallow water equation (NSWE) solver built on the OP2 domain-specific language (DSL) for unstructured mesh computations. VOLNA-OP2 is unique among tsunami solvers in its support for several high-performance computing platforms: central processing units (CPUs), the Intel Xeon Phi, and graphics processing units (GPUs).			

Table A2. Usage of methods.

Abb.	Method	Usage
AMS	Accelerator Mass Spectrometry	To obtain radiocarbon ages
CFD	Computational Fluid Dynamics	As a part of OpenFOAM; model of FLOW3D; to solve a three-dimensional Reynolds Averaged Navier–Stokes equations; to investigate solitary wave-induced vertical and horizontal forces on coastal bridges; to predict flow character and dynamic loading profile from an idealized tsunami impact on a coastal community; to simulate impulse wave generation and propagation; to simulate a tsunami
CRS	Constant Rate of Supply method	To develop dates of tsunami deposits
DEM	Digital Elevation Models	To capture a shielding phenomenon created by the dense buildings; to generate images; for topographical data; to calculate finite difference grid; to calculate a bathymetry and derived seafloor attributes such as slope gradient; to evaluate a model; to generate an inundation zones
FAM	Finite Area Method	To address the problem of fluid information mapped from the three-dimensional space to the two-dimensional space
FCM	Fuzzy C-Means Clustering	As part of used method
FEM	Finite Element Mesh	To create a mesh
FFT	Fast Fourier Transform	To analyze data; to obtain value for equations
FVCF	Finite Volume with Characteristic Flux	As part of equations
FVM	Finite Volume Method	To compute the two-phase incompressible flow with the Navier–Stokes equations; as a solver; as a part of model
GKS	Gustafsson–Kreiss–Sundström stability theory	To evaluate penalization
GPR	Ground-Penetrating Radar	For characterizing the subsurface subsidence structure associated with sinkholes and reconstructing their deformational and tsunami deposit history; to trace extent and morphology
LSWE	Linear Shallow Water Equations	As a part of COMCOT; to calculate a tsunami
MAP	Maximum a Posteriori Values	To calculate an estimate of the maximum water surface elevation standard deviation; to characterize solution of the problem
MC	Monte Carlo	To combine a probability of occurrence of earthquake; to estimate a relative error; to evaluate an overall uncertainty in tsunami hazard; to generate a synthetic earthquake catalog; to sample a resulting posterior; to confirm robustness of the created index; to vary all uncertain input parameters have been randomly within the specified distribution

Table A2. *Cont.*

Abb.	Method	Usage
MOST	Method for Splitting Tsunamis	To simulate a tsunami; to simulate an earthquake-generated tsunami
MULES	Multidimensional Universal Limiter for Explicit Solution	To maintain boundedness of a volume fraction; to maintain boundedness of a volume fraction independent of the underlying numerical scheme, mesh structure, etc.
NSWE	Nonlinear Shallow Water Equations	To calculate a long wave propagation; to simulate protection of small islands; as a base for modified equations; as a governing equation; to describe a propagation problem; to perform numerical simulations of volcanic explosion resulting in a tsunami wave traveling across the water; to solve tsunami equations
PCA	Principal Component Analysis	For a dimensionality reduction; to select relevant variables
PIMPLE	Pressure Implicit with Splitting of Operator	For a pressure-velocity solver; to employ a pressure-velocity solver To solve a velocity and pressure
PISO	Pressure Implicit with Splitting of Operators	To obtain a pressure field; to solve RANS equations with a volume of fluid
PTHA	Probabilistic Tsunami Hazard Analysis	As based method for expanded method; for modeling a tsunami
SIMPLE	Semi-Implicit Method for Pres-sure-Linked Equations	As a part of PIMPLE
SPH	Smoothed Particle Hydrodynamics	As a based method for enchanted method; for wave propagation from off- to onshore; to simulate waves; to study the nature of flows for an extreme wave above and in the interior of gravel bedforms
SWE	Shallow Water Equations	As a base for a model; for modeling a tsunami with small numbers of observation points in more physically realistic settings; to calculate a model
VOF	Volume of Fluid	To capture a free surface; to obtain sea-level or mudslide interface location; to figure out the role of vegetation of finite width in energy reduction of flood flow; to track the free surface between two fluids

Table A3. Relationship among tools and research domains.

	Agisoft	Amira	ANSYS	ArcGIS	CALIB	COMCOT	Delft3D	DSAS	Fledermaus	FLOW3D	Gambit	GeoClaw	Geowave	HAZUS	HydroSed2D	ICEM	MATLAB	MB-System	OpenFOAM	OsiriX DICOM	Qgis	R-studio	reflexW	SPAD	tsunami-2d	VOLNA	Total	
Applications Geosciences, Multidisciplinary	0	0	0	0	0	0	0	0	0	0	0	0	0	0	1	0	0	0	0	0	0	0	0	0	0	0	1	
Computer Science, Interdisciplinary	0	0	0	0	0	0	0	0	0	0	0	1	0	0	1	0	0	0	0	0	0	0	0	0	0	0	0	2
Computer Science, Theory, and Methods	0	0	0	0	0	0	0	0	0	0	0	0	0	0	0	0	1	0	0	0	0	0	0	0	0	0	1	
Engineering, Civil	0	0	3	1	0	1	1	0	0	0	0	0	0	1	0	0	3	0	10	0	1	0	0	0	0	0	21	
Engineering, Environmental	0	0	0	1	0	0	0	0	0	0	0	0	0	0	0	0	0	0	1	0	0	0	0	0	0	0	2	
Engineering, Geological	1	0	0	2	0	0	0	0	0	0	1	0	0	0	0	0	0	0	0	0	0	0	0	0	0	0	4	
Engineering, Marine	0	0	2	0	0	0	1	0	0	0	0	0	0	0	0	0	2	0	8	0	1	0	0	0	0	0	14	
Engineering, Mechanical	0	0	0	0	0	0	0	0	0	0	0	0	0	0	1	0	0	0	2	0	0	0	0	0	0	0	3	
Engineering, Multidisciplinary	3	0	1	0	0	0	0	0	0	0	0	0	0	0	0	1	1	0	2	0	0	0	0	0	0	0	8	
Engineering, Ocean	0	0	2	1	0	1	2	0	0	0	0	0	0	1	0	0	4	0	16	0	1	0	0	0	0	0	28	
Environmental Sciences	0	0	0	0	0	1	0	0	0	0	0	0	0	0	0	0	0	1	2	1	0	0	0	0	0	0	5	
Geography, Physical	0	0	0	0	3	0	0	1	0	0	0	0	0	0	0	0	0	1	0	0	0	1	0	0	0	0	6	
Geochemistry and Geophysics	0	0	0	0	1	3	0	0	0	0	0	1	0	0	0	0	3	0	0	0	0	0	0	0	0	0	8	
Geology	0	0	0	0	2	0	0	0	0	0	0	0	0	0	0	0	0	0	0	0	1	0	0	0	0	0	3	
Geosciences, Multidisciplinary	0	1	0	8	8	5	1	1	1	0	1	3	1	0	0	0	4	2	3	0	3	0	1	1	0	0	44	
Imaging Science and Photographic Technology	0	0	0	0	0	0	0	0	0	0	0	0	0	0	0	0	0	0	0	1	0	0	0	0	0	0	1	
Materials Science, Multidisciplinary	0	0	1	0	0	0	0	0	0	0	0	0	0	0	0	0	0	0	0	0	0	0	0	0	0	0	1	
Mathematics, Applied	0	0	0	1	0	0	0	0	0	0	0	0	0	0	0	0	1	0	0	0	0	0	0	0	0	1	3	
Mathematics, Interdisciplinary Applications	0	0	0	0	0	0	0	0	0	0	0	0	0	0	0	0	1	0	1	0	0	0	0	0	0	0	2	
Mechanics	0	0	1	0	0	0	0	0	0	0	0	0	0	0	0	1	1	0	2	0	0	0	0	0	0	0	5	
Meteorology and Atmospheric Sciences	0	0	0	3	1	3	1	0	0	0	0	1	1	0	0	0	2	0	3	0	0	0	0	1	0	0	16	
Multidisciplinary Sciences	0	0	0	2	1	0	1	0	0	0	0	0	0	0	0	0	0	0	0	1	0	0	0	0	0	1	6	
Nuclear Science and Technology	0	0	0	0	0	0	0	0	0	0	0	0	0	0	0	0	0	0	0	0	0	0	0	0	1	0	1	
Oceanography	2	0	2	5	3	1	1	0	1	1	0	1	0	0	0	0	3	1	8	0	1	0	0	0	1	0	31	
Physics, Fluids, and Plasmas	0	0	1	0	0	0	0	0	0	0	0	0	0	0	0	0	0	0	1	0	0	0	0	0	0	0	2	
Physics, Mathematical	0	0	0	0	0	0	0	0	0	0	0	0	0	0	0	0	1	0	0	0	0	0	0	0	0	0	1	
Remote Sensing	0	0	0	0	0	0	0	0	0	0	0	0	0	0	0	0	0	0	0	1	0	0	0	0	0	0	1	
Statistics and Probability	0	0	0	0	0	0	0	0	0	0	0	0	0	0	0	0	1	0	0	0	0	0	0	0	0	0	1	
Water Resources	0	0	0	4	1	3	1	0	0	0	0	1	1	0	0	0	1	0	6	0	1	0	0	1	0	0	20	
Total	6	1	13	28	20	18	9	2	2	1	2	8	3	2	2	3	29	5	65	1	11	1	2	3	2	2		

Appendix B. Module Formation of Tsunami: Equations

The following equations are taken from the model created in the Stella Professional software. In this modeling toolkit, the variables are defined using pseudocode.

$$\text{phase velocity of the wave} = \sqrt{\text{gravitational acceleration} * \text{water depth}} \quad (\text{A1})$$

$$\text{wave period} = \frac{\text{wave length}}{\text{phase velocity of the wave}} \quad (\text{A2})$$

$$\text{wave length} = \text{phase velocity of the wave} * \text{wave period} \quad (\text{A3})$$

$$\text{wave height} = \frac{1}{\sqrt{\text{water depth}}} \quad (\text{A4})$$

$$\text{estimated runup} = (\text{maximum wave amplitude})^{\frac{4}{5}} * (\text{gauge location water depth})^{\frac{1}{5}} \quad (\text{A5})$$

$$\text{runup factor} = \frac{\text{wave aplitude}}{\text{maximum runup height}} \quad (\text{A6})$$

$$\text{maximum runup height} = 2.831 * \sqrt{\text{cot inclination of the coast}} * (\text{tsunami wave height before shoaling})^{\frac{5}{4}} \quad (\text{A7})$$

$$\text{Imamura lida magnitude scale} = \frac{\ln \text{maximum runup height}}{\ln 2} \quad (\text{A8})$$

$$\text{flow velocity of the runup} = (\text{inundation depth})^{0.7} * \sqrt{\text{tan inclination of the water surface}} * \text{Manning's roughness coefficient} \quad (\text{A9})$$

$$\text{inundation distance} = \frac{0.06 * \left(\frac{\text{wave height at the shore}}{3}\right)}{(\text{Manning's roughness coefficient})^2} \quad (\text{A10})$$

$$\text{loss in wave height per meter of inundation distance} = \frac{167 * (\text{Manning's roughness coefficient})^2}{(\text{wave height at the shore})^{\frac{1}{3}}} + (5 * \sin \text{ground slope}) \quad (\text{A11})$$

$$\begin{aligned} \text{wave runup} = & (1 + \text{experimental constant}) * \frac{1+2*\text{experimental constant}}{(2*(\text{experimental constant})^2)} \\ & * (1 \\ & + \left(8 * \text{gravitational acceleration} * \frac{(\text{Manning's roughness coefficient})^2}{0.91} * (\text{experimental constant})^2 \right. \\ & \left. * \text{ground slope} * (\text{wave height at the shore})^{\frac{1}{3}}\right)) \end{aligned} \quad (\text{A12})$$

Appendix C. Module Defense Elements: Equations

$$\text{velocity within rubble mound} = \text{experimental coefficient} * \sqrt{2 * \text{gravitational acceleration} * h} \quad (\text{A13})$$

$$\text{surge force per unit width of the wall} = 4.5 * \text{density of seawater} * \text{gravitational acceleration} * (\text{surge height})^2 \quad (\text{A14})$$

$$\text{Gaussian distribution} = \text{tsunami height} * \exp\left(-\frac{(\text{time} - \text{rise time})^2}{\text{rise time}}\right) \quad (\text{A15})$$

$$\begin{aligned} \text{weight of required armour} \\ = & \frac{\text{density of armour} * (\text{wave height})^3}{\text{empirically determined damage coefficient} * (\text{relative underwater density of armour} - 1)^3 * \cos \text{slope of structure}} \end{aligned} \quad (\text{A16})$$

References

1. Frequently Asked Questions. Available online: http://itic.ioc-unesco.org/index.php?option=com_content&view=article&id=1133&Itemid=2155 (accessed on 1 July 2023).
2. Nacházel, T.; Babič, F.; Baiguera, M.; Čech, P.; Husáková, M.; Mikulecký, P.; Mls, K.; Ponce, D.; Salmanidou, D.; Štekerová, K.; et al. Tsunami-Related Data: A Review of Available Repositories Used in Scientific Literature. *Water* **2021**, *13*, 2177. [CrossRef]
3. Tappin, D.R. The Generation of Tsunamis. In *Encyclopedia of Maritime and Offshore Engineering*; Carlton, J., Jukes, P., Choo, Y.S., Eds.; John Wiley & Sons, Ltd.: Chichester, UK, 2017; pp. 1–10. ISBN 978-1-118-47635-2.
4. Tsunamis. Available online: <https://www.who.int/westernpacific/health-topics/tsunamis> (accessed on 1 July 2023).
5. Monecke, K.; Finger, W.; Klarer, D.; Kongko, W.; McAdoo, B.G.; Moore, A.L.; Sudrajat, S.U. A 1000-Year Sediment Record of Tsunami Recurrence in Northern Sumatra. *Nature* **2008**, *455*, 1232–1234. [CrossRef]
6. Borrero, J.C. Field Survey of Northern Sumatra and Banda Aceh, Indonesia after the Tsunami and Earthquake of 26 December 2004. *Seismol. Res. Lett.* **2005**, *76*, 312–320. [CrossRef]
7. Macías, J.; Castro, M.J.; Ortega, S.; Escalante, C.; González-Vida, J.M. Performance Benchmarking of Tsunami-HySEA Model for NTHMP's Inundation Mapping Activities. *Pure Appl. Geophys.* **2017**, *174*, 3147–3183. [CrossRef]
8. López-Venegas, A.M.; Horrillo, J.; Pampell-Manis, A.; Huérfano, V.; Mercado, A. Advanced Tsunami Numerical Simulations and Energy Considerations by Use of 3D–2D Coupled Models: The October 11, 1918, Mona Passage Tsunami. *Pure Appl. Geophys.* **2015**, *172*, 1679–1698. [CrossRef]
9. Wendt, J.; Oglesby, D.D.; Geist, E.L. Tsunamis and Splay Fault Dynamics. *Geophys. Res. Lett.* **2009**, *36*. [CrossRef]
10. Mulia, I.E.; Gusman, A.R.; Satake, K. Alternative to Non-Linear Model for Simulating Tsunami Inundation in Real-Time. *Geophys. J. Int.* **2018**, *214*, 2002–2013. [CrossRef]
11. Arcos, M.E.M.; LeVeque, R.J. Validating Velocities in the GeoClaw Tsunami Model Using Observations near Hawaii from the 2011 Tohoku Tsunami. *Pure Appl. Geophys.* **2015**, *172*, 849–867. [CrossRef]
12. Palupi, L.S. Psychological Preparedness for Disaster of Coastal Communities: A Systematic Review. *IOP Conf. Ser. Earth Environ. Sci.* **2021**, *649*, 012032. [CrossRef]
13. Fernandez, A.; Black, J.; Jones, M.; Wilson, L.; Salvador-Carulla, L.; Astell-Burt, T.; Black, D. Flooding and Mental Health: A Systematic Mapping Review. *PLoS ONE* **2015**, *10*, e0119929. [CrossRef]
14. PRISMA. The PRISMA 2020 Statement. Available online: <https://www.bmj.com/lookup/doi/10.1136/bmj.n71> (accessed on 1 July 2023).
15. Adobe. Available online: <https://www.adobe.com/> (accessed on 1 July 2023).
16. VOSviewer. Available online: <https://www.vosviewer.com/> (accessed on 1 July 2023).
17. Williams, A.; Kennedy, S.; Philipp, F.; Whiteman, G. Systems Thinking: A Review of Sustainability Management Research. *J. Clean. Prod.* **2017**, *148*, 866–881. [CrossRef]
18. Bureš, V.; Rácz, F. Identification of Sustainability Key Factors Based on Capturing Dominant Feedbacks of Behavioural Stereotypes in Socio-Economic Systems. *Systems* **2017**, *5*, 42. [CrossRef]
19. Barlas, Y. Formal Aspects of Model Validity and Validation in System Dynamics. *Syst. Dyn. Rev.* **1996**, *12*, 183–210. [CrossRef]
20. Liu, X.; Liu, C.; Zhu, X.; He, Y.; Wang, Q.; Wu, Z. 3D Modeling and Mechanism Analysis of Breaking Wave-Induced Seabed Scour around Monopile. *Math. Probl. Eng.* **2020**, *2020*, 1–17. [CrossRef]
21. Qin, X.; Motley, M.; LeVeque, R.; Gonzalez, F.; Mueller, K. A Comparison of a Two-Dimensional Depth-Averaged Flow Model and a Three-Dimensional RANS Model for Predicting Tsunami Inundation and Fluid Forces. *Nat. Hazards Earth Syst. Sci.* **2018**, *18*, 2489–2506. [CrossRef]
22. Autret, R.; Dodet, G.; Fichaut, B.; Suarez, S.; David, L.; Leckler, F.; Ardhuin, F.; Ammann, J.; Grandjean, P.; Allemand, P.; et al. A Comprehensive Hydro-Geomorphologic Study of Cliff-Top Storm Deposits on Banneg Island during Winter 2013–2014. *Mar. Geol.* **2016**, *382*, 37–55. [CrossRef]
23. Xiong, Y.; Liang, Q.; Park, H.; Cox, D.; Wang, G. A Deterministic Approach for Assessing Tsunami-Induced Building Damage through Quantification of Hydrodynamic Forces. *Coast. Eng.* **2019**, *144*, 1–14. [CrossRef]
24. Bellotti, G. A Modal Decomposition Method for the Analysis of Long Waves Amplification at Coastal Areas. *Coast. Eng.* **2020**, *157*, 103632. [CrossRef]
25. Abril, J.M.; Periañez, R. A Modelling Study on Tsunami Propagation in the Red Sea: Historical Events, Potential Hazards and Spectral Analysis. *Ocean Eng.* **2017**, *134*, 1–12. [CrossRef]
26. Yao, Y.; Jia, M.; Mao, D.; Deng, Z.; Liu, X. A Numerical Investigation of the Reduction of Solitary Wave Runup by A Row of Vertical Slotted Piles. *China Ocean Eng.* **2020**, *34*, 10–20. [CrossRef]
27. Tan, H.; Ruffini, G.; Heller, V.; Chen, S. A Numerical Landslide-Tsunami Hazard Assessment Technique Applied on Hypothetical Scenarios at Es Vedrà, Offshore Ibiza. *J. Mar. Sci. Eng.* **2018**, *6*, 111. [CrossRef]
28. Knighton, J.; Bastidas, L.A. A Proposed Probabilistic Seismic Tsunami Hazard Analysis Methodology. *Nat. Hazards* **2015**, *78*, 699–723. [CrossRef]
29. Horrillo, J.; Wood, A.; Kim, G.-B.; Parambath, A. A Simplified 3-D Navier-Stokes Numerical Model for Landslide-Tsunami: Application to the Gulf of Mexico: A Simplified 3-D Tsunami Numerical Model. *J. Geophys. Res. Ocean* **2013**, *118*, 6934–6950. [CrossRef]

30. Kevlahan, N.K.-R.; Dubos, T.; Aechtner, M. Adaptive Wavelet Simulation of Global Ocean Dynamics Using a New Brinkman Volume Penalization. *Geosci. Model. Dev.* **2015**, *8*, 3891–3909. [[CrossRef](#)]
31. Aristodemo, F.; Tripepi, G.; Algeri Ferraro, D.; Veltri, P. An Experimental and Numerical Study on Solitary Wave Loads at Cylinders near the Bed. *Ocean Eng.* **2020**, *195*, 106747. [[CrossRef](#)]
32. Wang, X.; Liu, P.L.-F. An Explicit Finite Difference Model for Simulating Weakly Nonlinear and Weakly Dispersive Waves over Slowly Varying Water Depth. *Coast. Eng.* **2011**, *58*, 173–183. [[CrossRef](#)]
33. Völker, D.; Scholz, F.; Geersen, J. Analysis of Submarine Landsliding in the Rupture Area of the 27 February 2010 Maule Earthquake, Central Chile. *Mar. Geol.* **2011**, *288*, 79–89. [[CrossRef](#)]
34. Flouri, E.T.; Kalligeris, N.; Alexandrakakis, G.; Kampanis, N.A.; Synolakis, C.E. Application of a Finite Difference Computational Model to the Simulation of Earthquake Generated Tsunamis. *Appl. Numer. Math.* **2013**, *67*, 111–125. [[CrossRef](#)]
35. Restrepo, A.J.D. Assessing the Effect of Sea-Level Change and Human Activities on a Major Delta on the Pacific Coast of Northern South America: The Patía River. *Geomorphology* **2012**, *151–152*, 207–223. [[CrossRef](#)]
36. Giraldi, L.; Le Maître, O.P.; Mandli, K.T.; Dawson, C.N.; Hoteit, I.; Knio, O.M. Bayesian Inference of Earthquake Parameters from Buoy Data Using a Polynomial Chaos-Based Surrogate. *Comput. Geosci.* **2017**, *21*, 683–699. [[CrossRef](#)]
37. Stefanakis, T.S.; Contal, E.; Vayatis, N.; Dias, F.; Synolakis, C.E. Can Small Islands Protect Nearby Coasts from Tsunamis? An Active Experimental Design Approach. *Proc. R. Soc. A* **2014**, *470*, 20140575. [[CrossRef](#)]
38. Abril-Hernández, J.M.; Perriáñez, R.; O'Connor, J.E.; Garcia-Castellanos, D. Computational Fluid Dynamics Simulations of the Late Pleistocene Lake Bonneville Flood. *J. Hydrol.* **2018**, *561*, 1–15. [[CrossRef](#)]
39. Mehrotra, A.; Singh, K.K.; Nigam, M.J.; Pal, K. Detection of Tsunami-Induced Changes Using Generalized Improved Fuzzy Radial Basis Function Neural Network. *Nat. Hazards* **2015**, *77*, 367–381. [[CrossRef](#)]
40. Amante, C.J. Estimating Coastal Digital Elevation Model Uncertainty. *J. Coast. Res.* **2018**, *34*, 1382. [[CrossRef](#)]
41. Mitsui, J.; Matsumoto, A.; Hanzawa, M.; Nadaoka, K. Estimation Method of Armor Stability Against Tsunami Overtopping Caisson Breakwater Based on Overflow Depth. *Coast. Eng. J.* **2016**, *58*, 1640019–1–1640019–20. [[CrossRef](#)]
42. Zhu, D.; Dong, Y. Experimental and 3D Numerical Investigation of Solitary Wave Forces on Coastal Bridges. *Ocean Eng.* **2020**, *209*, 107499. [[CrossRef](#)]
43. Förster, A.; Ellis, R.G.; Henrich, R.; Krastel, S.; Kopf, A.J. Geotechnical Characterization and Strain Analyses of Sediment in the Mauritania Slide Complex, NW-Africa. *Mar. Pet. Geol.* **2010**, *27*, 1175–1189. [[CrossRef](#)]
44. Puga-Bernabéu, Á.; Beaman, R.J.; Webster, J.M.; Thomas, A.L.; Jacobsen, G. Gloria Knolls Slide: A Prominent Submarine Landslide Complex on the Great Barrier Reef Margin of North-Eastern Australia. *Mar. Geol.* **2017**, *385*, 68–83. [[CrossRef](#)]
45. Bourget, J.; Zaragosi, S.; Ellouz-Zimmermann, S.; Ducassou, E.; Prins, M.A.; Garlan, T.; Lanfumey, V.; Schneider, J.-L.; Rouillard, P.; Giraudeau, J. Highstand vs. Lowstand Turbidite System Growth in the Makran Active Margin: Imprints of High-Frequency External Controls on Sediment Delivery Mechanisms to Deep Water Systems. *Mar. Geol.* **2010**, *274*, 187–208. [[CrossRef](#)]
46. Smith, D.E.; Davies, M.H.; Brooks, C.L.; Mighall, T.M.; Dawson, S.; Rea, B.R.; Jordan, J.T.; Holloway, L.K. Holocene Relative Sea Levels and Related Prehistoric Activity in the Forth Lowland, Scotland, United Kingdom. *Quat. Sci. Rev.* **2010**, *29*, 2382–2410. [[CrossRef](#)]
47. Baumann, J.; Chaumillon, E.; Bertin, X.; Schneider, J.-L.; Guillot, B.; Schmutz, M. Importance of Infragravity Waves for the Generation of Washover Deposits. *Mar. Geol.* **2017**, *391*, 20–35. [[CrossRef](#)]
48. Ali, A.; Pasha, G.A.; Ghani, U.; Ahmed, A.; Abbas, F.M. Investigating Role of Vegetation in Protection of Houses during Floods. *Civ. Eng. J.* **2019**, *5*, 2598–2613. [[CrossRef](#)]
49. Torres, C.E.; Calisto, I.; Figueroa, D. Magnetic Signals at Easter Island During the 2010 and 2015 Chilean Tsunamis Compared with Numerical Models. *Pure Appl. Geophys.* **2019**, *176*, 3167–3183. [[CrossRef](#)]
50. Polonia, A.; Bonatti, E.; Camerlenghi, A.; Lucchi, R.G.; Panieri, G.; Gasperini, L. Mediterranean Megaturbidite Triggered by the AD 365 Crete Earthquake and Tsunami. *Sci. Rep.* **2013**, *3*, 1285. [[CrossRef](#)] [[PubMed](#)]
51. Dutykh, D.; Clamond, D. Modified Shallow Water Equations for Significantly Varying Seabeds. *Appl. Math. Model.* **2016**, *40*, 9767–9787. [[CrossRef](#)]
52. Jing, H.; Zhang, H.; Yuen, D.A.; Shi, Y. Numerical Analysis of Wave Hazards in a Harbor. *Sci. China Earth Sci.* **2012**, *55*, 1554–1564. [[CrossRef](#)]
53. Jiang, C.; Liu, X.; Yao, Y.; Deng, B. Numerical Investigation of Solitary Wave Interaction with a Row of Vertical Slotted Piles on a Sloping Beach. *Int. J. Nav. Archit. Ocean Eng.* **2019**, *11*, 530–541. [[CrossRef](#)]
54. Sarjamee, S.; Nistor, I.; Mohammadian, A. Numerical Investigation of the Influence of Extreme Hydrodynamic Forces on the Geometry of Structures Using OpenFOAM. *Nat. Hazards* **2017**, *87*, 213–235. [[CrossRef](#)]
55. Li, J.; Qi, M.; Fuhrman, D.R. Numerical Modeling of Flow and Morphology Induced by a Solitary Wave on a Sloping Beach. *Appl. Ocean Res.* **2019**, *82*, 259–273. [[CrossRef](#)]
56. Ruffini, G.; Heller, V.; Briganti, R. Numerical Modelling of Landslide-Tsunami Propagation in a Wide Range of Idealised Water Body Geometries. *Coast. Eng.* **2019**, *153*, 103518. [[CrossRef](#)]
57. Wijetunge, J.J. Numerical Simulation and Field Survey of Inundation Due to 2004 Indian Ocean Tsunami in Trincomalee, Sri Lanka. *Nat. Hazards* **2010**, *54*, 177–192. [[CrossRef](#)]

58. Ulvrová, M.; Paris, R.; Kelfoun, K.; Nomikou, P. Numerical Simulations of Tsunamis Generated by Underwater Volcanic Explosions at Karymskoye Lake (Kamchatka, Russia) and Kolumbo Volcano (Aegean Sea, Greece). *Nat. Hazards Earth Syst. Sci.* **2014**, *14*, 401–412. [[CrossRef](#)]
59. Zhang, H.; Zhang, M.; Ji, Y.; Wang, Y.; Xu, T. Numerical Study of Tsunami Wave Run-up and Land Inundation on Coastal Vegetated Beaches. *Comput. Geosci.* **2019**, *132*, 9–22. [[CrossRef](#)]
60. Kevlahan, N.K.-R.; Khan, R.; Protas, B. On the Convergence of Data Assimilation for the One-Dimensional Shallow Water Equations with Sparse Observations. *Adv. Comput. Math.* **2019**, *45*, 3195–3216. [[CrossRef](#)]
61. Douglas, S.; Nistor, I. On the Effect of Bed Condition on the Development of Tsunami-Induced Loading on Structures Using OpenFOAM. *Nat. Hazards* **2015**, *76*, 1335–1356. [[CrossRef](#)]
62. Bartzke, G.; Podszun, L.; Huhn, K. On the Role of Fluid Infiltration into Gravel Dunes—Using a 3D Numerical Model. *Mar. Geol.* **2016**, *380*, 231–244. [[CrossRef](#)]
63. San Pedro, L.; Babonneau, N.; Gutscher, M.-A.; Cattaneo, A. Origin and Chronology of the Augias Deposit in the Ionian Sea (Central Mediterranean Sea), Based on New Regional Sedimentological Data. *Mar. Geol.* **2017**, *384*, 199–213. [[CrossRef](#)]
64. Premasiri, R.; Styles, P.; Shrira, V.; Cassidy, N.; Schwenninger, J.-L. OSL Dating and GPR Mapping of Palaeotsunami Inundation: A 4000-Year History of Indian Ocean Tsunamis as Recorded in Sri Lanka. *Pure Appl. Geophys.* **2015**, *172*, 3357–3384. [[CrossRef](#)]
65. Cheff, I.; Nistor, I.; Palermo, D. Pedestrian Evacuation Modelling of a Canadian West Coast Community from a Near-Field Tsunami Event. *Nat. Hazards* **2019**, *98*, 229–249. [[CrossRef](#)]
66. Zhang, X.; Niu, X. Probabilistic Tsunami Hazard Assessment and Its Application to Southeast Coast of Hainan Island from Manila Trench. *Coast. Eng.* **2020**, *155*, 103596. [[CrossRef](#)]
67. Juran, L.; Adams, E.A.; Prajapati, S. Purity, Pollution, and Space: Barriers to Latrine Adoption in Post-Disaster India. *Environ. Manag.* **2019**, *64*, 456–469. [[CrossRef](#)] [[PubMed](#)]
68. Sraj, I.; Mandli, K.T.; Knio, O.M.; Dawson, C.N.; Hoteit, I. Quantifying Uncertainties in Fault Slip Distribution during the Tōhoku Tsunami Using Polynomial Chaos. *Ocean Dyn.* **2017**, *67*, 1535–1551. [[CrossRef](#)]
69. Triantafyllou, I.; Novikova, T.; Charalampakis, M.; Fokaefs, A.; Papadopoulos, G.A. Quantitative Tsunami Risk Assessment in Terms of Building Replacement Cost Based on Tsunami Modelling and GIS Methods: The Case of Crete Isl., Hellenic Arc. *Pure Appl. Geophys.* **2019**, *176*, 3207–3225. [[CrossRef](#)]
70. Chen, G.-Y.; Liu, C.-C.; Wijetunge, J.J.; Wang, Y.-F. Reciprocal Green's Functions and the Quick Forecast of Submarine Landslide Tsunamis. *Nat. Hazards Earth Syst. Sci.* **2020**, *20*, 771–781. [[CrossRef](#)]
71. Reinhardt, E.G.; Nairn, R.B.; Lopez, G. Recovery Estimates for the Río Cruces after the May 1960 Chilean Earthquake. *Mar. Geol.* **2010**, *269*, 18–33. [[CrossRef](#)]
72. Stefanakis, T.S.; Xu, S.; Dutykh, D.; Dias, F. Run-up Amplification of Transient Long Waves. *Quart. Appl. Math.* **2015**, *73*, 177–199. [[CrossRef](#)]
73. Álvarez-Gómez, J.A.; Aniel-Quiroga, Í.; González, M.; Olabarrieta, M.; Carreño, E. Scenarios for Earthquake-Generated Tsunamis on a Complex Tectonic Area of Diffuse Deformation and Low Velocity: The Alboran Sea, Western Mediterranean. *Mar. Geol.* **2011**, *284*, 55–73. [[CrossRef](#)]
74. Çağatay, M.N.; Erel, L.; Bellucci, L.G.; Polonia, A.; Gasperini, L.; Eriş, K.K.; Sancar, Ü.; Biltekin, D.; Uçarkuş, G.; Ülgen, U.B.; et al. Sedimentary Earthquake Records in the İzmit Gulf, Sea of Marmara, Turkey. *Sediment. Geol.* **2012**, *282*, 347–359. [[CrossRef](#)]
75. Dahanayake, K.; Kulasena, N.; Ravi Prasad, G.V.; Dutta, K.; Ray, D.K. Sedimentological and ¹⁴C Dating Studies of Past Tsunami Events in Southern Sri Lanka. *Nat. Hazards* **2012**, *63*, 197–209. [[CrossRef](#)]
76. Vött, A.; Lang, F.; Brückner, H.; Gaki-Papanastassiou, K.; Maroukian, H.; Papanastassiou, D.; Giannikos, A.; Hadler, H.; Handl, M.; Ntageretzi, K.; et al. Sedimentological and Geoarchaeological Evidence of Multiple Tsunamigenic Imprint on the Bay of Palairos-Pogonia (Akarnania, NW Greece). *Quat. Int.* **2011**, *242*, 213–239. [[CrossRef](#)]
77. Yakupoğlu, N.; Uçarkuş, G.; Kadir Eriş, K.; Henry, P.; Namık Çağatay, M. Sedimentological and Geochemical Evidence for Seismoturbidite Generation in the Kumburgaz Basin, Sea of Marmara: Implications for Earthquake Recurrence along the Central High Segment of the North Anatolian Fault. *Sediment. Geol.* **2019**, *380*, 31–44. [[CrossRef](#)]
78. Stiros, S.C.; Blackman, D.J. Seismic Coastal Uplift and Subsidence in Rhodes Island, Aegean Arc: Evidence from an Uplifted Ancient Harbour. *Tectonophysics* **2014**, *611*, 114–120. [[CrossRef](#)]
79. Ma, Z.; Zhou, T.; Sun, J.; Zhai, G. Simulation on Tsunami-like Solitary Wave Run-up around a Conical Island Using a Modified Mass Source Method. *Eng. Appl. Comput. Fluid Mech.* **2019**, *13*, 849–859. [[CrossRef](#)]
80. Sarfaraz, M.; Pak, A. SPH Numerical Simulation of Tsunami Wave Forces Impinged on Bridge Superstructures. *Coast. Eng.* **2017**, *121*, 145–157. [[CrossRef](#)]
81. Yang, W.; Lai, W.; Zhu, Q.; Zhang, C.; Li, F. Study on Generation Mechanism of Vertical Force Peak Values on T-Girder Attacked by Tsunami Bore. *Ocean Eng.* **2020**, *196*, 106782. [[CrossRef](#)]
82. Webster, J.M.; George, N.P.J.; Beaman, R.J.; Hill, J.; Puga-Bernabéu, Á.; Hinestrosa, G.; Abbey, E.A.; Daniell, J.J. Submarine Landslides on the Great Barrier Reef Shelf Edge and Upper Slope: A Mechanism for Generating Tsunamis on the North-East Australian Coast? *Mar. Geol.* **2016**, *371*, 120–129. [[CrossRef](#)]
83. Fabregat, I.; Gutiérrez, F.; Roqué, C.; Zarroca, M.; Linares, R.; Comas, X.; Guerrero, J.; Carbonel, D. Subsidence Mechanisms and Sedimentation in Alluvial Sinkholes Inferred from Trenching and Ground Penetrating Radar (GPR). Implications for Subsidence and Flooding Hazard Assessment. *Quat. Int.* **2019**, *525*, 1–15. [[CrossRef](#)]

84. Gylfadóttir, S.S.; Kim, J.; Helgason, J.K.; Brynjólfsson, S.; Höskuldsson, Á.; Jóhannesson, T.; Harbitz, C.B.; Løvholt, F. The 2014 L Ake A Skja Rockslide-induced Tsunami: Optimization of Numerical Tsunami Model Using Observed Data. *JGR Ocean* **2017**, *122*, 4110–4122. [[CrossRef](#)]
85. Higman, B.; Shugar, D.H.; Stark, C.P.; Ekström, G.; Koppes, M.N.; Lynett, P.; Dufresne, A.; Haeussler, P.J.; Geertsema, M.; Gulick, S.; et al. The 2015 Landslide and Tsunami in Taan Fiord, Alaska. *Sci. Rep.* **2018**, *8*, 12993. [[CrossRef](#)] [[PubMed](#)]
86. Xing, A.; Xu, Q.; Zhu, Y.; Zhu, J.; Jiang, Y. The August 27, 2014, Rock Avalanche and Related Impulse Water Waves in Fuquan, Guizhou, China. *Landslides* **2016**, *13*, 411–422. [[CrossRef](#)]
87. Dall’Osso, F.; Dominey-Howes, D.; Moore, C.; Summerhayes, S.; Withycombe, G. The Exposure of Sydney (Australia) to Earthquake-Generated Tsunamis, Storms and Sea Level Rise: A Probabilistic Multi-Hazard Approach. *Sci. Rep.* **2014**, *4*, 7401. [[CrossRef](#)] [[PubMed](#)]
88. Xie, P.; Chu, V.H. The Forces of Tsunami Waves on a Vertical Wall and on a Structure of Finite Width. *Coast. Eng.* **2019**, *149*, 65–80. [[CrossRef](#)]
89. Creach, A.; Pardo, S.; Guillotreau, P.; Mercier, D. The Use of a Micro-Scale Index to Identify Potential Death Risk Areas Due to Coastal Flood Surges: Lessons from Storm Xynthia on the French Atlantic Coast. *Nat. Hazards* **2015**, *77*, 1679–1710. [[CrossRef](#)]
90. Qin, X.; Motley, M.R.; Marafi, N.A. Three-Dimensional Modeling of Tsunami Forces on Coastal Communities. *Coast. Eng.* **2018**, *140*, 43–59. [[CrossRef](#)]
91. Álvarez-Gómez, J.A.; Aniel-Quiroga, Í.; Gutiérrez-Gutiérrez, O.Q.; Larreynaga, J.; González, M.; Castro, M.; Gavidia, F.; Aguirre-Ayerbe, I.; González-Riancho, P.; Carreño, E. Tsunami Hazard Assessment in El Salvador, Central America, from Seismic Sources through Flooding Numerical Models. *Nat. Hazards Earth Syst. Sci.* **2013**, *13*, 2927–2939. [[CrossRef](#)]
92. DeDontney, N.; Rice, J.R. Tsunami Wave Analysis and Possibility of Splay Fault Rupture During the 2004 Indian Ocean Earthquake. *Pure Appl. Geophys.* **2012**, *169*, 1707–1735. [[CrossRef](#)]
93. Cariotlet, J.-M. Use of High Water Marks and Eyewitness Accounts to Delineate Flooded Coastal Areas: The Case of Storm Johanna (10 March 2008) in Brittany, France. *Ocean Coast. Manag.* **2010**, *53*, 679–690. [[CrossRef](#)]
94. Boshenyatov, B.; Zhiltsov, K. Vortex Suppression of Tsunami-like Waves by Underwater Barriers. *Ocean Eng.* **2019**, *183*, 398–408. [[CrossRef](#)]
95. Reynolds, M.H.; Courtot, K.N.; Berkowitz, P.; Storlazzi, C.D.; Moore, J.; Flint, E. Will the Effects of Sea-Level Rise Create Ecological Traps for Pacific Island Seabirds? *PLoS ONE* **2015**, *10*, e0136773. [[CrossRef](#)]
96. Benazir, Syamsidik; Idris, Y.; Putra, N. Connecting Community’s Perspectives on Tsunami Risk to Anticipated Future Tsunamis: A Reflection from a Progress of Tsunami Preparedness from a Coastal Community in Aceh-Indonesia after 19 Years of the 2004 Indian Ocean Tsunami. *Geoenviron. Disasters* **2023**, *10*, 21. [[CrossRef](#)]
97. Rauter, M.; Hosse, L.; Mulligan, R.; Take, W.; Lovholt, F. Numerical Simulation of Impulse Wave Generation by Idealized Landslides with OpenFOAM. *Coast. Eng.* **2021**, *165*, 103815. [[CrossRef](#)]
98. Nemati, F.; Leonard, L.; Thomson, R.; Lintern, G.; Kouhi, S. Numerical Modeling of a Potential Landslide-Generated Tsunami in the Southern Strait of Georgia. *Nat. Hazards* **2023**, *117*, 2029–2054. [[CrossRef](#)]
99. Guo, R.; Lo, P. Numerical Investigation on Solitary Wave Interaction with a Vertical Cylinder over a Viscous Mud Bed. *Water* **2022**, *14*, 1135. [[CrossRef](#)]
100. Attili, T.; Heller, V.; Triantafyllou, S. A Numerical Investigation of Tsunamis Impacting Dams. *Coast. Eng.* **2021**, *169*, 103942. [[CrossRef](#)]
101. Pakoksung, K.; Suppasri, A.; Imamura, F. Probabilistic Tsunami Hazard Analysis of Inundated Buildings Following a Subaqueous Volcanic Explosion Based on the 1716 Tsunami Scenario in Taal Lake, Philippines. *Geosciences* **2021**, *11*, 92. [[CrossRef](#)]
102. Song, Y.; Jia, J.; Liu, H.; Chen, F.; Fang, Q. Numerical Study on Tsunami Force on Coastal Bridge Decks with Superelevation. *J. Mar. Sci. Eng.* **2023**, *11*, 824. [[CrossRef](#)]
103. Elsheikh, N.; Nistor, I.; Azimi, A.; Mohammadian, A. Tsunami-Induced Bore Propagating over a Canal-Part 1: Laboratory Experiments and Numerical Validation. *Fluids* **2022**, *7*, 213. [[CrossRef](#)]
104. Rahuman, S.; Ismail, A.; Varghese, S.; Toworfe, G. Comparative Study of Flow Patterns around Rhizophora and Avicennia Mangrove Roots Using Computational Fluid Dynamics Simulation. *Adv. Mater. Sci. Eng.* **2022**, *2022*, 8992513. [[CrossRef](#)]
105. Amina; Tanaka, N. Numerical Investigation of 3D Flow Properties around Finite Emergent Vegetation by Using the Two-Phase Volume of Fluid (VOF) Modeling Technique. *Fluids* **2022**, *7*, 175. [[CrossRef](#)]
106. Liu, J.; Hayatdavoodi, M. On Solitary Wave Breaking and Impact on a Horizontal Deck. *J. Mar. Sci. Eng.* **2023**, *11*, 1033. [[CrossRef](#)]
107. Paulin, D.; Jasra, A.; Beskos, A.; Crisan, D. A 4D-Var Method with Flow-Dependent Background Covariances for the Shallow-Water Equations. *Stat. Comput.* **2022**, *32*, 65. [[CrossRef](#)]
108. Kalligeris, N.; Skanavis, V.; Charalampakis, M.; Melis, N.; Voukouvalas, E.; Annunziato, A.; Synolakis, C. Field Survey of the 30 October 2020 Samos (Aegean Sea) Tsunami in the Greek Islands. *Bull. Earthq. Eng.* **2022**, *20*, 7873–7905. [[CrossRef](#)] [[PubMed](#)]
109. Tong, S.; Vanden-Eijnden, E.; Stadler, G. Estimating Earthquake-Induced Tsunami Height Probabilities without Sampling. *Pure Appl. Geophys.* **2023**, *180*, 1587–1597. [[CrossRef](#)]
110. Dai, X.; Schneider-Muntau, B.; Fellin, W.; Franco, A.; Gems, B. Engineering-Geological Analysis of a Subaerial Landslide in Taan Fiord, Alaska. *Remote Sens.* **2021**, *13*, 4258. [[CrossRef](#)]
111. Madden, I.; Marras, S.; Suckale, J. Leveraging Google’s Tensor Processing Units for Tsunami-Risk Mitigation Planning in the Pacific Northwest and Beyond. *Geosci. Model Dev.* **2023**, *16*, 3479–3500. [[CrossRef](#)]

112. Yuan, Y.; Li, H.; Wei, Y.; Shi, F.; Wang, Z.; Hou, J.; Wang, P.; Xu, Z. Probabilistic Tsunami Hazard Assessment (PTHA) for Southeast Coast of Chinese Mainland and Taiwan Island. *J. Geophys. Res. Solid Earth* **2021**, *126*, e2020JB020344. [CrossRef]
113. Celikbas, B.; Tufekci-Enginar, D.; Dogan, G.; Kolat, C.; Santini, M.; Annunziato, A.; Necmioglu, O.; Yalciner, A.; Suzen, M. Pedestrian Evacuation Time Calculation against Tsunami Hazard for Southern Coasts of Bodrum Peninsula. *Nat. Hazards* **2023**, *119*, 243–260. [CrossRef]
114. Zengaffinen-Morris, T.; Urgeles, R.; Lovholt, F. On the Inference of Tsunami Uncertainties From Landslide Run-Out Observations. *J. Geophys. Res. Ocean* **2022**, *127*, e2021JC018033. [CrossRef]
115. Mokhtarzadeh, G.; Basirat, S.; Bazargan, J.; Delavari, E. Impulse Wave Generation: A Comparison of Landslides of Block and Granular Masses by Coupled Lagrangian Tracking Using VOF over a Set Mesh. *Water Supply* **2022**, *22*, 510–526. [CrossRef]
116. Mu, D.; Chen, L.; Ning, D. Modeling Impact Load on a Vertical Cylinder in Dam-Break Flows. *J. Mar. Sci. Eng.* **2023**, *11*, 932. [CrossRef]
117. Dai, Z.; Li, X.; Lan, B. Three-Dimensional Modeling of Tsunami Waves Triggered by Submarine Landslides Based on the Smoothed Particle Hydrodynamics Method. *J. Mar. Sci. Eng.* **2023**, *11*, 2015. [CrossRef]
118. Zhang, M.; Huang, W.; Qiu, J. A High-Order Well-Balanced Positivity-Preserving Moving Mesh DG Method for the Shallow Water Equations With Non-Flat Bottom Topography. *J. Sci. Comput.* **2021**, *87*, 88. [CrossRef]
119. Ersoy, H.; Sünnetci, M.; Karahan, M.; Perinçek, D. 3D Simulations of Impulse Waves Originating from Concurrent Landslides near an Active Fault Using FLOW-3D Software: A Case Study of Cetin Dam Reservoir (Southeast Turkey). *Bull. Eng. Geol. Environ.* **2022**, *81*, 267. [CrossRef]
120. Paris, A.; Heinrich, P.; Abadie, S. Landslide Tsunamis: Comparison between Depth-Averaged and Navier-Stokes Models. *Coast. Eng.* **2021**, *170*, 104022. [CrossRef]
121. Lo Re, C.; Manno, G.; Basile, M.; Ferrotto, M.; Cavaleri, L.; Ciraolo, G. Tsunami Vulnerability Evaluation for a Small Ancient Village on Eastern Sicily Coast. *J. Mar. Sci. Eng.* **2022**, *10*, 268. [CrossRef]
122. Takegawa, N.; Sawada, Y.; Furuichi, N. Strategic Coastal Dike Shape for Enhanced Tsunami Overflow Reduction. *PLoS ONE* **2023**, *18*, e0292930. [CrossRef] [PubMed]
123. Papadopoulos, G.A.; Imamura, F. A Proposal for a New Tsunami Intensity Scale. *ITS Proc.* **2001**, *5*, 569–577.
124. The Engineering ToolBox. Available online: https://www.engineeringtoolbox.com/mannings-roughness-d_799.html (accessed on 1 July 2023).
125. Leone, F.; Lavigne, F.; Paris, R.; Denain, J.-C.; Vinet, F. A Spatial Analysis of the December 26th, 2004 Tsunami-Induced Damages: Lessons Learned for a Better Risk Assessment Integrating Buildings Vulnerability. *Appl. Geogr.* **2011**, *31*, 363–375. [CrossRef]
126. Rossetto, T.; Peiris, N.; Pomonis, A.; Wilkinson, S.M.; Del Re, D.; Koo, R.; Gallocher, S. The Indian Ocean Tsunami of December 26, 2004: Observations in Sri Lanka and Thailand. *Nat. Hazards* **2007**, *42*, 105–124. [CrossRef]
127. Ghobarah, A.; Saatcioglu, M.; Nistor, I. The Impact of the 26 December 2004 Earthquake and Tsunami on Structures and Infrastructure. *Eng. Struct.* **2006**, *28*, 312–326. [CrossRef]
128. Valencia, N.; Gardi, A.; Gauraz, A.; Leone, F.; Guillande, R. New Tsunami Damage Functions Developed in the Framework of SCHEMA Project: Application to European-Mediterranean Coasts. *Nat. Hazards Earth Syst. Sci.* **2011**, *11*, 2835–2846. [CrossRef]
129. Heger, M.P.; Neumayer, E. The Impact of the Indian Ocean Tsunami on Aceh's Long-Term Economic Growth. *J. Dev. Econ.* **2019**, *141*, 102365. [CrossRef]
130. Kweifio-Okai, C. Where Did the Indian Ocean Tsunami Aid Money Go? In *The Guardian*; Kings Place: London, UK, 2014.
131. Takagi, H.; Tomiyasu, R.; Oyake, T.; Araki, T.; Mori, K.; Matsubara, Y.; Ninomiya, Y.; Takata, Y. Tsunami Intrusion through Port Breakwaters Enclosed with Self-Elevating Seawalls. *Ocean Eng.* **2020**, *199*, 107028. [CrossRef]
132. Nakashima, S.; Takayama, T.; Obara, K.; Kawasaki, T.; Kurokawa, F.; Onodera, T. Performance Based Design of Vertically Telescopic Breakwater for Protection from Tsunami. *J. Jpn. Soc. Civ. Eng. Ser. B2 Coast. Eng.* **2011**, *67*, I_786–I_790. [CrossRef] [PubMed]
133. Kamphuis, J.W. *Introduction to Coastal Engineering and Management*; World Scientific: Singapore, 2020; Volume 48, ISBN 9811208018.
134. Coastal Engineering Research Center. *Shore Protection Manual*, 4th ed.; Coastal Engineering Research Center: Ford Belvoir, VA, USA, 1984.
135. Esteban, M.; Thao, N.D.; Takagi, H.; Jayaratne, R.; Mikami, T.; Shibayama, T. Stability of Breakwaters against Tsunami Attack. In *Handbook of Coastal Disaster Mitigation for Engineers and Planners*; Elsevier: Amsterdam, The Netherlands, 2015; pp. 293–323. ISBN 978-0-12-801060-0.
136. Van der Meer, J.W. Stability of Breakwater Armour Layers—Design Formulae. *Coast. Eng.* **1987**, *11*, 219–239. [CrossRef]
137. Scheel, H.J. New Type of Tsunami Barrier. *Nat. Hazards* **2014**, *70*, 951–956. [CrossRef]
138. Levin, B.W.; Nosov, M. *Physics of Tsunamis*; Springer: Berlin/Heidelberg, Germany, 2009; Volume 327.
139. Srinivas, H.; Nakagawa, Y. Environmental Implications for Disaster Preparedness: Lessons Learnt from the Indian Ocean Tsunami. *J. Environ. Manag.* **2008**, *89*, 4–13. [CrossRef] [PubMed]
140. Marras, S.; Mandli, K.T. Modeling and Simulation of Tsunami Impact: A Short Review of Recent Advances and Future Challenges. *Geosciences* **2020**, *11*, 5. [CrossRef]
141. Belliazzi, S.; Lignola, G.P.; Di Ludovico, M.; Prota, A. Preliminary Tsunami Analytical Fragility Functions Proposal for Italian Coastal Residential Masonry Buildings. *Structures* **2021**, *31*, 68–79. [CrossRef]

142. Cavaleri, L.; Ciraolo, G.; Ferrotto, M.F.; La Loggia, G.; Lo Re, C.; Manno, G. Masonry Structures Subjected to Tsunami Loads: Modeling Issues and Application to a Case Study. *Structures* **2020**, *27*, 2192–2207. [[CrossRef](#)]
143. Del Zoppo, M.; Wijesundara, K.; Rossetto, T.; Dias, P.; Baiguera, M.; Di Ludovico, M.; Thamboo, J.; Prota, A. Influence of Exterior Infill Walls on the Performance of RC Frames under Tsunami Loads: Case Study of School Buildings in Sri Lanka. *Eng. Struct.* **2021**, *234*, 111920. [[CrossRef](#)]
144. Ferrotto, M.F.; Cavaleri, L. Masonry Structures: A Proposal of Analytical Generation of Fragility Functions for Tsunami Impact—Application to the Mediterranean Coasts. *Eng. Struct.* **2021**, *242*, 112463. [[CrossRef](#)]
145. Medina, S.; Lizarazo-Marriaga, J.; Estrada, M.; Koshimura, S.; Mas, E.; Adriano, B. Tsunami Analytical Fragility Curves for the Colombian Pacific Coast: A Reinforced Concrete Building Example. *Eng. Struct.* **2019**, *196*, 109309. [[CrossRef](#)]
146. Mei, H.; Guo, A. Performance of RC Shear Keys on Coastal Bridges under Multi-Hazard Actions of Earthquake and Sequent Tsunami. *Structures* **2024**, *65*, 106672. [[CrossRef](#)]
147. Oddo, M.C.; Asteris, P.G.; Cavaleri, L. Monte Carlo Analysis of Masonry Structures under Tsunami Action: Reliability of Lognormal Fragility Curves and Overall Uncertainty Prediction. *Structures* **2024**, *63*, 106421. [[CrossRef](#)]
148. Xu, J.-G.; Wu, G.; Feng, D.-C.; Fan, J.-J. Probabilistic Multi-Hazard Fragility Analysis of RC Bridges under Earthquake-Tsunami Sequential Events. *Eng. Struct.* **2021**, *238*, 112250. [[CrossRef](#)]
149. Birta, L.G.; Arbez, G. *Modelling and Simulation: Exploring Dynamic System Behaviour*; Simulation Foundations, Methods and Applications; Springer International Publishing: Cham, Switzerland, 2019; ISBN 978-3-030-18868-9.
150. Shuto, N.; Fujima, K. A Short History of Tsunami Research and Countermeasures in Japan. *Proc. Jpn. Acad. Ser. B* **2009**, *85*, 267–275. [[CrossRef](#)]

Disclaimer/Publisher’s Note: The statements, opinions and data contained in all publications are solely those of the individual author(s) and contributor(s) and not of MDPI and/or the editor(s). MDPI and/or the editor(s) disclaim responsibility for any injury to people or property resulting from any ideas, methods, instructions or products referred to in the content.